arXiv:1703.00676v2 [cs.LG] 10 Mar 2017

# A Unifying View of Explicit and Implicit Feature Maps for Structured Data: Systematic Studies of Graph Kernels*

**Nils M. Kriege** NILS.KRIEGE@TU-DORTMUND.DE
*Department of Computer Science*
*TU Dortmund University*
*44221 Dortmund, Germany*

**Marion Neumann** M.NEUMANN@WUSTL.EDU
*Department of Computer Science and Engineering*
*Washington University in St. Louis*
*St. Louis, MO 63130, USA*

**Christopher Morris** CHRISTOPHER.MORRIS@TU-DORTMUND.DE
**Kristian Kersting** KRISTIAN.KERSTING@TU-DORTMUND.DE
**Petra Mutzel** PETRA.MUTZEL@TU-DORTMUND.DE
*Department of Computer Science*
*TU Dortmund University*
*44221 Dortmund, Germany*

## Abstract

Non-linear kernel methods can be approximated by fast linear ones using suitable explicit feature maps allowing their application to large scale problems. To this end, explicit feature maps of kernels for vectorial data have been extensively studied. As many real-world data is structured, various kernels for complex data like graphs have been proposed. Indeed, many of them directly compute feature maps. However, the kernel trick is employed when the number of features is very large or the individual vertices of graphs are annotated by real-valued attributes.

Can we still compute explicit feature maps efficiently under these circumstances? Triggered by this question, we investigate how general convolution kernels are composed from base kernels and construct corresponding feature maps. We apply our results to widely used graph kernels and analyze for which kernels and graph properties computation by explicit feature maps is feasible and actually more efficient. In particular, we derive feature maps for random walk and subgraph matching kernels and apply them to real-world graphs with discrete labels. Thereby, our theoretical results are confirmed experimentally by observing a phase transition when comparing running time with respect to label diversity, walk lengths and subgraph size, respectively. Moreover, we derive approximative, explicit feature maps for state-of-the-art kernels supporting real-valued attributes including the GraphHopper and Graph Invariant kernels. In extensive experiments we show that our approaches often achieve a classification accuracy close to the exact methods based on the kernel trick, but require only a fraction of their running time.

**Keywords:** graph kernels, feature maps, random walk kernel, structured data, supervised learning

∗. A preliminary version of this paper appeared in the proceedings of the IEEE International Conference on Data Mining (ICDM) in 2014 (Kriege, Neumann, Kersting, and Mutzel, 2014).

©2017 Nils M. Kriege, Marion Neumann, Christopher Morris, Kristian Kersting, and Petra Mutzel.

## 1. Introduction

Analyzing complex data is becoming more and more important. In numerous application domains, e.g., chem- and bioinformatics, neuroscience, or image and social network analysis, the data is structured and hence can naturally be represented as graphs. To achieve successful learning we need to exploit the rich information inherent in the graph structure and the annotations of vertices and edges. A popular approach to mining structured data is to design graph kernels measuring the similarity between graphs. The graph kernel can then be plugged into a kernel machine, such as support vector machine or Gaussian process, for efficient learning and prediction.

The kernel-based approach to predictive graph mining requires a positive semidefinite (p.s.d.) kernel function between graphs. Graphs, composed of labeled vertices and edges possibly enriched with continuous attributes, however, are not fixed-length vectors but rather complicated data structures, and thus standard kernels cannot be used. Instead, the general strategy to design graph kernels is to decompose graphs into small substructures among which kernels are defined following the concept of convolution kernels due to Haussler (1999). The graph kernel itself is then a combination of the kernels between the possibly overlapping parts. Hence the various graph kernels proposed in the literature mainly differ in the way the parts are constructed and in the similarity measure used to compare them. Most of them can be seen as instances of convolution kernels (Vishwanathan et al., 2010). Moreover, existing graph kernels also differ in their ability to exploit annotations, which may be categorical labels or real-valued attributes on the vertices and edges.

We remind basic facts on kernels, which have decisive implications on several computational aspects. A *kernel* on a non-empty set $\mathcal{X}$ is a positive semidefinite function $k : \mathcal{X} \times \mathcal{X} \to \mathbb{R}$. Equivalently, a function $k$ is a kernel if there is a *feature map* $\phi : \mathcal{X} \to \mathcal{H}$ to a real Hilbert space $\mathcal{H}$ with inner product $\langle \cdot, \cdot \rangle$, such that $k(x, y) = \langle \phi(x), \phi(y) \rangle$ for all $x$ and $y$ in $\mathcal{X}$. This equivalence yields two algorithmic strategies to compute kernels on graphs:

(i) One way is functional computation, e.g., from closed-form expressions. In this case the feature map is not necessarily known and the feature space may be of infinite dimension. Therefore, we refer to this approach closely related to the famous kernel trick as *implicit* computation.
(ii) The other strategy is to compute the feature map $\phi(G)$ for each graph $G$ *explicitly* to obtain the kernel values from the dot product between pairs of feature vectors. These feature vectors commonly count how often certain substructures occur in a graph.

Linear kernel methods based on explicit feature maps can often be implemented efficiently and are therefore preferred over their kernelized counterparts recently in practice. When feature maps are computed explicitly, the structured data is essentially transformed into vectorial data in a preprocessing step. Unique advantages of the implicit computation on the other hand are that

(i) kernels for composed objects can be combined of established kernels on their parts exploiting well-known closure properties of kernels;
(ii) the number of possible features may be high—in theory infinite—while the function remains polynomial-time computable.

Previously proposed graph kernels that are computed implicitly exploit at least one of the above mentioned advantages. Graph kernels computed by explicit feature maps do not allow to specify base kernels for parts like continuous vertex annotations, but scale to large graphs and datasets. We review concrete graph kernels with respect to this difference in Section 2 and proceed by summarizing our contribution.

### 1.1 Our Contribution

So far, previous work introducing novel graph kernels followed one of the strategies for computation. In contrast, we are interested in analyzing and comparing the computation schemes. We study under which conditions the computation of an explicit mapping from graphs to *finite-dimensional* feature spaces is feasible. To achieve our goal, we review closure properties of kernels and the corresponding feature maps with a focus on the size and sparsity of the feature vectors. Building on this we derive explicit feature maps for convolution kernels and assess how the properties of the graph in combination with the properties of the base kernel affect the running time. We theoretically analyze both methods of computation and identify a trade-off between running time and flexibility. We apply these results to obtain new algorithms for explicit graph kernel computation. We introduce the class of weighted vertex kernels and show that it generalizes state-of-the-art kernels for graphs with continuous attributes, namely the GraphHopper kernel (Feragen et al., 2013) and an instance of the Graph Invariant kernels (Orsini et al., 2015). We derive approximative, explicit feature maps for both based on approximate feature maps for the base kernels.

Then, we derive explicit computation schemes for random walk kernels (Gärtner et al., 2003; Vishwanathan et al., 2010), subgraph matching kernels (Kriege and Mutzel, 2012), and shortest-path kernels (Borgwardt and Kriegel, 2005). We compare efficient algorithms for the explicit and implicit computation of these kernels experimentally. Our product graph based computation of the walk kernel fully supports arbitrary vertex and edge kernels and exploits their sparsity. Further, we present the first explicit computation scheme for walk-based kernels. Given this, we are finally able to experimentally compare the running times of both computation strategies systematically with respect to the label diversity, data set size, and substructure size, i.e., walk length and subgraph size. As it turns out, there exists a computational phase transition for walk and subgraph kernels. Our experimental results for weighted vertex kernels show that their computation by explicit feature maps is feasible and provides a viable alternative even when comparing graphs with continuous attributes.

#### 1.1.1 EXTENSION OF THE CONFERENCE PAPER

The present paper is a significant extension of a previously published conference paper (Kriege et al., 2014). In the following we list the main contributions that were not included in the conference version.

**Feature maps of composed kernels.** We review closure properties of kernels, the corresponding feature maps and the size and sparsity of the feature vectors. Based on this, we obtain explicit feature maps for convolution kernels with arbitrary base kernels. This generalizes the result of the conference paper, where binary base kernel were considered.

**Weighted vertex kernels.** We introduce weighted vertex kernels generalizing two kernels for attributed graphs.

**Application of explicit feature maps.** We derive explicit feature maps for weighted vertex kernels and the shortest-path kernel (Borgwardt and Kriegel, 2005) supporting arbitrary base kernels for the comparison of attributes.

**Experimental evaluation.** We largely extended our evaluation, which now includes experiments for the novel computation schemes of graph kernels as well as a comparison between a graphlet kernel and the subgraph matching kernel (Kriege and Mutzel, 2012).

### 1.2 Outline

The article is organized as follows. In Section 2 we discuss related work and proceed by fixing the notation in Section 3. In Section 4, we discuss the computation of explicit and implicit kernels. Section 5 reviews closure properties of kernels and the corresponding feature maps. Moreover, we derive feature maps for the convolution kernel. Although the analysis and results presented in Sections 4 and 5 are valid for kernels in general, we give concrete examples arising in the domain of graph data. Subsequently, we derive feature maps for the shortest-path graph kernel, discuss the graphlet and the subgraph matching kernel, introduce the weighted vertex kernel and derive approximate feature maps. Moreover, we derive feature maps for the fixed length walk kernel and discuss different computation schemes. Section 7 presents the results of our experimental evaluation.

## 2. Related Work

In the following we review existing graph kernels based on explicit or implicit computation. For random walk kernels implicit computation schemes based on product graphs have been proposed. The product graph $G_\times$ has a vertex for each pair of vertices in the original graphs. Two vertices in the product graph are neighbors if the corresponding vertices in the original graphs were both neighbors as well. Product graphs have some nice properties making them suitable for the computation of graph kernels. First, the adjacency matrix $A_\times$ of a product graph is the Kronecker product of the adjacency matrices $A$ and $A'$ of the original graphs, i.e., $A_\times = A \otimes A'$, same holds for the weight matrix $W_\times$ when employing an edge kernel. Further, there is a one-to-one correspondence between walks on the product graph and simultaneous walks on the original graphs, cf. (Gärtner et al., 2003). The *random walk kernel* introduced by Vishwanathan et al. (2010) is now given by $K(G,H) = \sum_{l=0}^{\infty} \mu_l q_\times^\top W_\times^l p_\times$, where $p_\times$ and $q_\times$ are starting and stopping probability distributions and $\mu_l$ coefficients such that the sum converges. Several variations of the random walk kernel have been introduced in the literature. Instead of considering weights or probabilities, the geometric random walk kernel introduced by Gärtner et al. (2003) counts the number of matching walks. Other variants of random walk kernels have been proposed, cf. (Kashima et al., 2003; Mahé et al., 2004; Borgwardt et al., 2005; Harchaoui and Bach, 2007; Kang et al., 2012). See also (Sugiyama and Borgwardt, 2015) for some recent theoretical results on random walk kernels. Another substructure used to measure the similarity among graphs are shortest paths. Borgwardt and Kriegel (2005) proposed the *shortest-path kernel*, which compares two graphs based on vertex pairs with similar shortest-path lengths. The *GraphHopper kernel* compares the vertices encountered while hopping along shortest paths (Feragen et al., 2013). The above mentioned approaches support graphs with continuous attributes, further kernels for this application exist (Orsini et al., 2015; Su et al., 2016). Also computed via a product graph, the *subgraph matching kernel* compares subgraphs of small size allowing to rate mappings between them according to vertex and edge kernels (Kriege and Mutzel, 2012).

Avoiding the construction of potentially huge product graphs, explicit feature maps for graph kernels can often be computed more memory efficient and also faster. The features are typically counts or indicators of occurrences of substructures of particular sizes. The *graphlet kernel*, for example, counts induced subgraphs of size $k \in \{3,4,5\}$ of unlabeled graphs according to $K(G,H) = \mathbf{f}_G^\top \mathbf{f}_H$, where $\mathbf{f}_G$ and $\mathbf{f}_H$ are the count features of $G$ and $H$, respectively, cf. (Shervashidze et al., 2009). The *cyclic pattern kernel* measures the occurrence of cyclic and tree patterns and maps the graphs to pattern indicator features which are independent of the pattern frequency, cf. (Horváth et al., 2004).

The *Weisfeiler-Lehman subtree kernel* counts label-based subtree-patterns, cf. (Shervashidze et al., 2011), according to $K_d(G, H) = \sum_{i=1}^{h} K(G_i, H_i)$, where $K(G_i, H_i) = \langle \mathbf{f}_G^{(i)} \mathbf{f}_H^{(i)} \rangle$ and $\mathbf{f}_G^{(i)}$ is a feature vector counting subtree-patterns in $G$ of depth $i$. A subtree-pattern is a tree rooted at a particular vertex where each level contains the neighbors of its parent vertex; the same vertices can appear repeatedly. Other graph kernels on subtree-patterns have been proposed in the literature (Ramon and Gärtner, 2003; Harchaoui and Bach, 2007; Bai et al., 2015; Hido and Kashima, 2009). In a similar spirit, the *propagation kernel* iteratively counts similar label or attribute distributions to create an explicit feature map for efficient kernel computation (Neumann et al., 2016).

The large amount of recently introduced graph kernels indicates that machine learning on structured data is both considerably difficult and important. Surprisingly, none of the above introduced kernels is flexible enough to consider any kind of vertex and edge information while still being fast and memory efficient across arbitrary graph databases. The following observation is crucial. Graph kernels supporting complex annotations typically use implicit computation schemes and do not scale well. Whereas graphs with discrete labels are efficiently compared by graph kernels based on explicit feature maps. Recently the *hash graph kernel framework* (Morris et al., 2016) has been proposed to obtain efficient kernels for graphs with continuous labels from those proposed for discrete ones. The idea is to iteratively turn continuous attributes into discrete labels using randomized hash functions. A drawback of the approach is that so-called *independent $k$-hash families* must be known to guarantee that the approach approximates attribute comparisons by the kernel $k$. In practice locality-sensitive hashing is used, which does not provide this guarantee, but still achieves promising results. Apart from this approach no results on explicit feature maps for kernels on graphs with continuous attributes are known. However, explicit feature maps of kernels for vectorial data have been studied extensively. Starting with the seminal work by Rahimi and Recht (2008), explicit feature maps of various popular kernels have been proposed, cf. (Vedaldi and Zisserman, 2012; Kar and Karnick, 2012; Pham and Pagh, 2013, and references therein). We build on this line of work to obtain kernels for graphs, where individual vertices and edges are annotated by vectorial data. In contrast to the hash graph kernel framework our goal is to lift the known approximation results for kernels on vectorial data to kernels for graphs annotated with vector data.

## 3. Preliminaries

An *(undirected) graph* $G$ is a pair $(V, E)$ with a finite set of *vertices* $V$ and a set of *edges* $E \subseteq \{\{u, v\} \subseteq V \mid u \neq v\}$. We denote the set of vertices and the set of edges of $G$ by $V(G)$ and $E(G)$, respectively. For ease of notation we denote the edge $\{u, v\}$ in $E(G)$ by $uv$ or $vu$. A graph $G' = (V', E')$ is a *subgraph* of a graph $G = (V, E)$ if $V' \subseteq V$ and $E' \subseteq E$. The subgraph $G'$ is said to be *induced* if $E' = \{uv \in E \mid u, v \in V'\}$ and we write $G' \subseteq G$. We denote the *neighborhood* of a vertex $v$ in $V(G)$ by $\mathrm{N}(v) = \{u \in V(G) \mid vu \in E(G)\}$.

A *labeled graph* is a graph $G$ endowed with an *label function* $\tau \colon V(G) \to \Sigma$, where $\Sigma$ is a finite alphabet. We say that $\tau(v)$ is the *label* of $v$ for $v$ in $V(G)$. An *attributed graph* is a graph $G$ endowed with a function $\tau \colon V(G) \to \mathbb{R}^d$, $d \in \mathbb{N}$, and we say that $\tau(v)$ is the *attribute* of $v$. We denote the base kernel for comparing vertex labels and attributes by $k_V$ and, for short, write $k_V(u, v)$ instead of $k_V(\tau(u), \tau(v))$. The above definitions directly extend to graphs, where edges have labels or attributes and we denote the base kernel by $k_E$. We refer to $k_V$ and $k_E$ as *vertex kernel* and *edge kernel*, respectively.

For a vector $v$ in $\mathbb{R}^d$, we denote by $\mathsf{nz}(v)$ be the set of indices of the non-zero components of $v$ and let $\mathsf{nnz}(v) = |\mathsf{nz}(v)|$ the number of non-zero components.

## 4. Kernel Methods and Kernel Computation

Kernel methods supporting kernel functions are often slower than linear ones based on explicit feature maps assuming feature vectors are of a manageable size. This is for example the case for support vector machines, which classify objects according to their location w.r.t. a hyperplane. When computing feature maps explicitly, the normal vector of the hyperplane can be constructed explicitly as well and classification requires computing a single dot product only. The running time for this, essentially depends on number of (non-zero) components of the feature vectors. Using implicit computation the number of kernel computations required depends on the number of support vectors defining the hyperplane. Moreover, the running time for training a support vector machine is linear assuming a constant number of non-zero components (Joachims, 2006). The example illustrates that implicit and explicit kernel computation have a significant effect on the running time of the kernel method at the higher level. In order to compare the running time of both strategies systematically without dependence on one specific kernel method, we study the running time to compute a kernel matrix, which stores the kernel values for all pairs of data objects.

### 4.1 Computing Kernel Matrices

Algorithm 1 generates the kernel matrix in a straightforward manner by directly computing the kernel functions, thus applying a mapping into feature space implicitly. Here, we assume that the procedure

**Algorithm 1:** Computation by implicit mapping into feature space.

**Input** : A set of graphs $\mathcal{D} = \{G_1, \ldots, G_n\}$.
**Output** : Symmetric $n \times n$ kernel matrix $\mathbf{K}$ with entries $k_{ij}$.

```
1 for i ← 1 to n do
2     for j ← i to n do
3         k_ij ← COMPUTEKERNEL(G_i, G_j)          ▷ k_ji = k_ij
4 return K
```

COMPUTEKERNEL does not internally generate the feature vectors of the two graphs passed as parameters to compute the kernel function, of course. While this would in principle be possible, it would involve computing the feature vector of every graph $\mathcal{O}(n)$ times. When explicit mapping is applied, the feature vectors can be generated initially once for each graph of the data set. Then the matrix is computed by taking the dot product between these feature vectors, cf. Algorithm 2. This approach is equivalent to computing the matrix product $\mathbf{F}^\top\mathbf{F}$, where $\mathbf{F}$ is the matrix obtained by row-wise concatenation of the feature vectors.

Both approaches differ in terms of running time, which depends on the complexity of the individual procedures that must be computed in the course of the algorithms.

**Proposition 1** *Algorithm 1 computes an $n \times n$ kernel matrix in time $\mathcal{O}(n^2\mathsf{T}_k)$, where $\mathsf{T}_k$ is the running time of* COMPUTEKERNEL *to compute a single kernel value.*

**Algorithm 2:** Computation by explicit mapping into feature space.

**Input** : A set of graphs $\mathcal{D} = \{G_1, \ldots, G_n\}$.
**Data** : Feature vectors $\Phi_i$ for $i \in \{1, \ldots, n\}$.
**Output** : Symmetric $n \times n$ kernel matrix $\mathbf{K}$ with entries $k_{ij}$.

```
for i ← 1 to n do
    Φ_i ← FEATUREMAP(G_i)                          ▷ Compute φ(G_i)
for i ← 1 to n do                                  ▷ Compute K = (Φ_1 ··· Φ_n)^⊤ (Φ_1 ··· Φ_n)
    for j ← i to n do
        k_ij ← DOTPRODUCT(Φ_i, Φ_j)                ▷ k_ji = k_ij
return K
```

**Proposition 2** *Algorithm 2 computes an $n \times n$ kernel matrix in time $\mathcal{O}(n\mathsf{T}_\phi + n^2\mathsf{T}_{dot})$, where $\mathsf{T}_\phi$ is the running time of* FEATUREMAP *to compute the feature vector for a single graph and $\mathsf{T}_{dot}$ the running time of* DOTPRODUCT *for computing the dot product between two feature vectors.*

Clearly, explicit computation can only be competitive with implicit computation, when the time $\mathsf{T}_{\text{dot}}$ is smaller than $\mathsf{T}_k$. In this case, however, even a time-consuming feature mapping $\mathsf{T}_\phi$ pays off with increasing data set size. The running time $\mathsf{T}_{\text{dot}}$, thus, is crucial for explicit computation and depends on the data structure used to store feature vectors.

### 4.2 Storing Feature Vectors

A common approach to define a feature map is to assign each possible feature to one dimension of the feature space. Then the feature vector of an object is obtained by counting the occurrences of all features in the object. Such feature vectors are typically sparse and many of the theoretically possible features do not occur at all in a specific data set. When considering the label sequences of walks in a molecular graph, for example, a label sequence `H=H` would correspond to a hydrogen atom with a double bond to another hydrogen atom. This does not occur in valid chemical structures, but cannot be excluded in advance without domain knowledge. This is exploited by sparse data structures for vectors and matrices, which expose running times depending on the number of non-zero components instead of the actual number of all components. One approach to realize a sparse data structure for feature vectors is to employ a hash table. In this case the function DOTPRODUCT$(\Phi_1, \Phi_2)$ can be computed in time $\mathsf{T}_{dot} = \mathcal{O}(\min\{\mathsf{nnz}(\Phi_1), \mathsf{nnz}(\Phi_2)\})$ in the average case.

## 5. Basic Kernels, Composed Kernels and Their Feature Maps

Graph kernels, in particular those supporting user-specified kernels for annotations, typically employ closure properties. This allows to decompose graphs into parts that are eventually the annotated vertices and edges. The graph kernel then is composed of base kernels applied to the annotations and annotated substructures, respectively.

We first consider the feature maps of basic kernels and then review closure properties of kernels and discuss how to obtain their feature maps. Some of the basic results on the construction of feature maps and their detailed proof can be found in the text book by Shawe-Taylor and Cristianini (2004).

Going beyond that, we discuss the sparsity of the obtained feature vectors in detail, which has an essential impact on efficiency in practice. The results are summarized in Table 1. As we will see in Section 5.1 a large number of components of feature vectors may be—and in practice often is—zero. This is exploited by sparse data structures for vectors and matrices, cf. Section 4.2. Indeed the running times we observed experimentally in Section 7 can only be explained taking the sparsity into account.

### 5.1 Dirac and Binary Kernels

We discuss feature maps for basic kernels often used for the construction of kernels on structured objects. The Dirac kernel $k_\delta$ on $\mathcal{X}$ is defined by $k_\delta(x, y) = 1$, if $x = y$ and 0 otherwise. It is well-known that $\phi : \mathcal{X} \to \{0, 1\}^{|\mathcal{X}|}$ with components indexed by $i \in \mathcal{X}$ and defined as $\phi(x)_i = 1$ if $i = x$, and 0 otherwise, is a feature map of the Dirac kernel.

More generally, we say a kernel $k$ on $\mathcal{X}$ is *binary* if $k(x, y)$ is either 0 or 1 for all $x, y \in \mathcal{X}$. Given a binary kernel, we refer to

$$\sim_k = \{(x, y) \in \mathcal{X} \times \mathcal{X} \mid k(x, y) = 1\}$$

as the relation on $\mathcal{X}$ *induced by* $k$. Next we will establish several properties of this relation, which will turn out to be useful for the construction of a feature map.

**Lemma 3** *Let $k$ be a binary kernel on $\mathcal{X}$, then $x \sim_k y \implies x \sim_k x$ holds for all $x, y \in \mathcal{X}$.*

**Proof** Assume there are $x, y \in \mathcal{X}$ such that $x \not\sim_k x$ and $x \sim_k y$. By the definition of $\sim_k$ we obtain $k(x, x) = 0$ and $k(x, y) = 1$. The symmetric kernel matrix obtained by $k$ for $X = \{x, y\}$ thus is either $\left(\begin{smallmatrix} 0 & 1 \\ 1 & 0 \end{smallmatrix}\right)$ or $\left(\begin{smallmatrix} 0 & 1 \\ 1 & 1 \end{smallmatrix}\right)$, where we assume that the first row and column is associated with $x$. Both matrices are not p.s.d. and, thus, $k$ is not a kernel contradicting the assumption. ■

**Lemma 4** *Let $k$ be a binary kernel on $\mathcal{X}$, then $\sim_k$ is a partial equivalence relation meaning that the relation $\sim_k$ is (i) symmetric, and (ii) transitive.*

**Proof** Property (i) follows from the fact that $k$ must be symmetric according to definition. Assume property (ii) does not hold. Then there are $x, y, z \in \mathcal{X}$ with $x \sim_k y \wedge y \sim_k z$ and $x \not\sim_k z$. Since $x \neq z$ must hold according to Lemma 3 we can conclude that $X = \{x, y, z\}$ are pairwise distinct. We consider a kernel matrix $\mathbf{K}$ obtained by $k$ for $X$ and assume that the first, second and third row as well as column is associated with $x$, $y$ and $z$, respectively. There must be entries $k_{12} = k_{21} = k_{23} = k_{32} = 1$ and $k_{13} = k_{31} = 0$. According to Lemma 3 the entries of the main diagonal $k_{11} = k_{22} = k_{33} = 1$ follow. Consider the coefficient vector $\mathbf{c}$ with $c_1 = c_3 = 1$ and $c_2 = -1$, we obtain $\mathbf{c}^\top \mathbf{K} \mathbf{c} = -1$. Hence, $\mathbf{K}$ is not p.s.d. and $k$ is not a kernel contradicting the assumption. ■

We use these results to construct a feature map for a binary kernel. We restrict our consideration to the set $\mathcal{X}_{\text{ref}} = \{x \in \mathcal{X} \mid x \sim_k x\}$, on which $\sim_k$ is an equivalence relation. The quotient set $\mathcal{Q}_k = \mathcal{X}_{\text{ref}}/\sim_k$ is the set of equivalence classes induced by $\sim_k$. Let $[x]_k$ denote the equivalence class of $x \in \mathcal{X}_{\text{ref}}$ under the relation $\sim_k$. Let $k_\delta$ be the Dirac kernel on the equivalence classes $\mathcal{Q}_k$, then $k(x, y) = k_\delta([x]_k, [y]_k)$ and we obtain the following result.

Table 1: Composed kernels, their feature map, dimension and sparsity. We assume $k = k_1, \ldots, k_D$ to be kernels with feature maps $\phi = \phi_1, \ldots, \phi_D$ of dimension $d = d_1, \ldots, d_D$.

| **Kernel** | **Feature Map** | **Dimension** | **Sparsity** |
|---|---|---|---|
| $k^\alpha(x,y) = \alpha k(x,y)$ | $\phi^\alpha(x) = \sqrt{\alpha}\phi(x)$ | $d$ | $\mathsf{nnz}(\phi(x))$ |
| $k^+(x,y) = \sum_{i=1}^D k_i(x,y)$ | $\phi^+(x) = \bigoplus_{i=1}^D \phi_i(x)$ | $\sum_{i=1}^D d_i$ | $\sum_{i=1}^D \mathsf{nnz}(\phi_i(x))$ |
| $k^\bullet(x,y) = \prod_{i=1}^D k_i(x,y)$ | $\phi^\bullet(x) = \bigotimes_{i=1}^D \phi_i(x)$ | $\prod_{i=1}^D d_i$ | $\prod_{i=1}^D \mathsf{nnz}(\phi_i(x))$ |
| $k^\times(X,Y) = \sum_{x\in X}\sum_{y\in Y} k(x,y)$ | $\phi^\times(X) = \sum_{x\in X} \phi(x)$ | $d$ | $\left\lvert\bigcup_{x\in X} \mathsf{nz}(\phi(x))\right\rvert$ |

**Proposition 5** *Let $k$ be a binary kernel with $\mathcal{Q}_k = \{Q_1, \ldots, Q_d\}$, then $\phi : \mathcal{X} \to \{0,1\}^d$ with $\phi(x)_i = 1$ if $Q_i = [x]_k$, and $0$ otherwise, is a feature map of $k$.*

### 5.2 Closure Properties

For a kernel $k$ on a non-empty set $\mathcal{X}$ the function $k^\alpha(x,y) = \alpha k(x,y)$ with $\alpha$ in $\mathbb{R}_{\geq 0}$ is again a kernel on $\mathcal{X}$. Let $\phi$ be a feature map of $k$, then $\phi^\alpha(x) = \sqrt{\alpha}\phi(x)$ is a feature map of $k^\alpha$. For addition and multiplication, we get the following result.

**Proposition 6 (Shawe-Taylor and Cristianini 2004, pp. 75 sqq.)** *Let $k_1, \ldots, k_D$ for $D > 0$ be kernels on $\mathcal{X}$ with feature maps $\phi_1, \ldots, \phi_D$ of dimension $d_1, \ldots, d_D$, respectively. Then*

$$k^+(x,y) = \sum_{i=1}^D k_i(x,y) \quad \textit{and} \quad k^\bullet(x,y) = \prod_{i=1}^D k_i(x,y)$$

*are again kernels on $\mathcal{X}$. Moreover,*

$$\phi^+(x) = \bigoplus_{i=1}^D \phi_i(x) \quad \textit{and} \quad \phi^\bullet(x) = \bigotimes_{i=1}^D \phi_i(x)$$

*are feature maps for $k^+$ and $k^\bullet$ of dimension $\sum_{i=1}^D d_i$ and $\prod_{i=1}^D d_i$, respectively. Here $\oplus$ denotes the concatenation of vectors and $\otimes$ the Kronecker product.*

**Remark 7** *In case of $k_1 = k_2 = \ldots = k_D$, we have $k^+(x,y) = Dk_1(x,y)$ and a $d_1$-dimensional feature map can be obtained. For $k^\bullet$ we have $k_1(x,y)^D$, which yet does not allow for a feature space of dimension smaller than $d_1^D$ in general.*

We state an immediate consequence of Proposition 6 regarding the sparsity of the obtained feature vectors explicitly.

**Corollary 8** *Let $k_1, \ldots, k_D$ and $\phi_1, \ldots, \phi_D$ be defined as above, then*

$$\mathsf{nnz}(\phi^+(x)) = \sum_{i=1}^D \mathsf{nnz}(\phi_i(x)) \quad \textit{and} \quad \mathsf{nnz}(\phi^\bullet(x)) = \prod_{i=1}^D \mathsf{nnz}(\phi_i(x)).$$

### 5.3 Kernels on Sets

In the following we derive an explicit mapping for kernels on finite sets. This result will be needed in the succeeding section for constructing an explicit feature map for the $R$-convolution kernel. Let $k$ be a base kernel on a set $U$, and let $X$ and $Y$ be finite subsets of $U$. Then the *cross product kernel* or *derived subset kernel* on $\mathcal{P}(U)$ is defined as

$$k^{\times}(X,Y) = \sum_{x \in Y} \sum_{y \in Y} \kappa(x,y)\,. \tag{1}$$

Let $\phi$ be a feature map of $\kappa$, then the function

$$\phi^{\times}(X) = \sum_{x \in X} \phi(x) \tag{2}$$

is a feature map of the cross product kernel (Shawe-Taylor and Cristianini, 2004, Proposition 9.42). In particular, the feature space of the cross product kernel corresponds to the feature space of the base kernel; both have the same dimension. For $\kappa = k_\delta$ the Dirac kernel $\phi^{\times}(X)$ maps the set $X$ to its characteristic vector, which has $|U|$ components and $|X|$ non-zero elements. When $\kappa$ is a binary kernel as discussed in Section 5 the number of components reduces to the number of equivalence classes of $\sim_\kappa$ and the number of non-zero elements becomes the number of cells in the quotient set $X/\!\sim_\kappa$. In general, we obtain the following result as an immediate consequence of Equation (2).

**Corollary 9** *Let $\phi^{\times}$ be the feature map of the crossproduct kernel and $\phi$ the feature map of its base kernel, then*

$$\mathsf{nnz}(\phi^{\times}(X)) = \left| \bigcup_{x \in X} \mathsf{nz}(\phi(x)) \right| .$$

A crucial observation is that the number of non-zero components of a feature vector depends on both, the cardinality and structure of the set $X$ and the feature map $\phi$ acting on the elements of $X$. In the worst-case each element of $X$ is mapped by $\phi$ to a feature vector with distinct non-zero components.

### 5.4 Convolution Kernels

Haussler (1999) proposed $R$-convolution kernels as a generic framework to define kernels between composite objects. In the following we derive feature maps for such kernels by using the results for basic operations introduced in the previous sections. Thereby, we generalize the result presented in (Kriege et al., 2014).

**Definition 10** *Suppose $x \in \mathcal{R} = \mathcal{R}_1 \times \cdots \times \mathcal{R}_n$ are the parts of $X \in \mathcal{X}$ according to some decomposition. Let $R \subseteq \mathcal{X} \times \mathcal{R}$ be a relation such that $(X,x) \in R$ if and only if $X$ can be decomposed into the parts $x$. Let $R(X) = \{x \mid (X,x) \in R\}$ and assume $R(X)$ is finite for all $X \in \mathcal{X}$. The* $R$-convolution kernel *is*

$$k^{\star}(X,Y) = \sum_{x \in R(X)} \sum_{y \in R(Y)} \underbrace{\prod_{i=1}^{n} \kappa_i(x_i,y_i)}_{\kappa(x,y)}, \tag{3}$$

*where $\kappa_i$ is a kernel on $\mathcal{R}_i$ for all $i \in \{1,\ldots,n\}$.*

Assume that we have explicit feature maps for the kernels $\kappa_i$. We first note that a feature map for $\kappa$ can be obtained from the feature maps for $\kappa_i$ by Proposition 6.[1] In fact, Equation (3) for arbitrary $n$ can be obtained from the case $n = 1$ for an appropriate choice of $\mathcal{R}_1$ and $k_1$ as noted by Shin and Kuboyama (2010). If we assume $\mathcal{R} = \mathcal{R}_1 = U$, the $R$-convolution kernel boils down to the crossproduct kernel and we have $k^\star(X, Y) = k^\times(R(X), R(Y))$, where both employ the same base kernel $\kappa$. We use this approach to develop explicit mapping schemes for graph kernels in the following. Let $\phi$ be a feature map for $\kappa$ of dimension $d$, then from Equation (2), we obtain an explicit mapping of dimension $d$ for the $R$-convolution kernel according to

$$\phi^\star(X) = \sum_{x \in R(X)} \phi(x)\,. \tag{4}$$

As discussed in Section 5.3 the sparsity of $\phi^\star(X)$ simultaneous depends on the number of parts and their relation in the feature space of $\kappa$.

Kriege et al. (2014) considered the special case that $\kappa$ is a binary kernel, cf. Section 5.1. From Proposition 5 and Equation (4) we directly obtain their result as special case.

**Corollary 11 (Kriege et al. (2014), Theorem 3)** *Let $k^\star$ be an $R$-convolution kernel with binary kernel $\kappa$ and $\mathcal{Q}_\kappa = \{Q_1, \ldots, Q_d\}$, then $\phi^\star : \mathcal{X} \to \mathbb{N}^d$ with $\phi(x)_i = |Q_i \cap X|$ is a feature map of $k^\star$.*

## 6. Application to Graph Kernels

We apply the results obtained in the previous section to graph kernels, which are a prominent example of kernels for structured data. A crucial observation of our study of feature maps for composed kernels is the following. The number of components of the feature vectors increases multiplicative under taking products of kernels; this also holds in terms of non-zero components. Unless feature vectors have few non-zero components, this operation is likely to be prohibitive in practice. However, if feature vectors have exactly one non-zero component like those associated with binary kernels, taking products of kernels is manageable by sparse data structures.

Indeed, this fact explains a recent observation in the development of graph kernels (Morris et al., 2016): Graphs with discrete labels, which can be adequately compared by the Dirac kernel, can be compared efficiently by graph kernels based on explicit feature maps. Whereas graph kernels supporting complex annotations use implicit computation schemes and do not scale well. Typically graph kernels are proposed with one method of computation, either implicit or explicit.

We first discuss two families of kernels for which both computation schemes have been considered previously and put them in the context of our systematic study. We then derive explicit computation schemes of three kernels, for which methods of implicit computation have been proposed. We empirically study both computation schemes for graph kernels confirming our theoretical results experimentally in fine detail in Section 7.

### 6.1 Explicit Computation for Graphs with Discrete Labels

We review two kernels for which both methods of computation have been used previously. The shortest-path kernel was proposed with an implicit computation scheme, but explicit methods of computation have been reported to be used for graphs with discrete labels. Subgraph or graphlet

1. Note that we may consider every kernel $\kappa_i$ on $\mathcal{R}_i$ as kernel $\kappa_i'$ on $\mathcal{R}$ by defining $\kappa_i'(x, y) = \kappa_i(x_i, y_i)$.

kernels have been proposed for unlabeled graphs or graphs with discrete labels. The subgraph matching kernel has been developed as an extension for attributed graphs.

#### 6.1.1 SHORTEST-PATH KERNEL

A classical kernel applicable to attributed graphs is the shortest-path kernel (Borgwardt and Kriegel, 2005). This kernel compares all shortest paths in two graphs according to their lengths and the vertex annotation of their endpoints. The shortest-path kernel is defined as

$$k^{\mathrm{SP}}(G,H) = \sum_{\substack{u,v \in V(G),\\ u \neq v}} \sum_{\substack{w,z \in V(H),\\ w \neq z}} k_V(u,w) \cdot k_E(d_{uv}, d_{wz}) \cdot k_V(v,z), \tag{5}$$

where $\kappa_V$ is a kernel comparing vertex labels of the respective starting and end vertices of the paths. Here, $d_{uv}$ denotes the length of a shortest path from $u$ to $v$ and $k_E$ is a kernel comparing path lengths with $k_E(d_{uv}, d_{wz}) = 0$ if $d_{uv} = \infty$ or $d_{wz} = \infty$.

Its computation is performed in two steps (Borgwardt and Kriegel, 2005): for each graph $G$ of the data set the complete graph $G'$ on the vertex set $V(G)$ is generated, where an edge $uv$ is annotated with the length of a shortest path from $u$ to $v$. The shortest-path kernel then is equivalent to the walk kernel with fixed length $\ell = 1$ between these transformed graphs, where the kernel essentially compares all pairs of edges. The kernel $k_E$ used to compare path lengths may, for example, be realized by the Brownian Bridge kernel (Borgwardt and Kriegel, 2005).

For the application to graphs with discrete labels a more efficient method of computation by explicit mapping has been reported by Shervashidze et al. (2011, Section 3.4.1). When $k_V$ and $k_E$ both are Dirac kernels, each component of the feature vector corresponds to a triple consisting of two vertex labels and a path length. This method of computation has been applied in several experimental comparisons, e.g., (Kriege and Mutzel, 2012; Morris et al., 2016). This feature map is directly obtained from our results in Section 5. It is as well rediscovered from our explicit computation schemes for fixed length walk kernels reported in Section 6.3. However, we can also derive explicit feature maps for non-trivial kernels $k_V$ and $k_E$. Then the dimension of the feature map increases due to the product of kernels, cf. Equation 5. We will study this and the effect on running time experimentally in Section 7.

#### 6.1.2 GRAPHLET, SUBGRAPH AND SUBGRAPH MATCHING KERNELS

Given two graphs $G$ and $H$ in $\mathcal{G}$, the *subgraph kernel* is defined as

$$k^{\subseteq}(G,H) = \sum_{G' \subseteq G} \sum_{H' \subseteq H} k_{\simeq}(G',H'), \tag{6}$$

where $k_{\simeq} : \mathcal{G} \times \mathcal{G} \to \{0,1\}$ is the isomorphism kernel, i.e., $k_{\simeq}(G',H') = 1$ if and only if $G'$ and $H'$ are isomorphic. A similar kernel was defined by Gärtner et al. (2003) and its computation was shown to be NP-hard. However, it is polynomial time computable when considering only subgraphs up to a fixed size. The subgraph kernel, cf. Equation (6), is easily identified as an instance of the crossproduct kernel, cf. Equation (1). The base kernel $k_{\simeq}$ is not the trivial Dirac kernel, but binary, cf. Section 5.1. The equivalence classes induced by $k_{\simeq}$ are referred to as isomorphism classes and distinguish subgraphs up to isomorphism. The feature map $\phi_{\subseteq}$ of $k^{\subseteq}$ maps a graph to a vector, where each component counts the number of occurrences of a specific graph as subgraph in $G$. Determining

the isomorphism class of a graph is known as *graph canonization problem* and well-studied. By solving the graph canonization problem instead of the graph isomorphism problem we obtain an explicit feature map for the subgraph kernel. Although graph canonization clearly is at least as hard as graph isomorphism, the number of canonizations required is linear in the number of subgraphs, while a quadratic number of isomorphism tests would be required for a single naïve computation of the kernel. The gap in terms of runtime even increases when computing a whole kernel matrix, cf. Section 4.1.

Indeed, the observations above are a key to several graph kernels recently proposed. The graphlet kernel (Shervashidze et al., 2009), also see Section 2, is an instance of the subgraph kernel and computed by explicit feature maps. However, only unlabeled graphs of small size are considered by the graphlet kernel, such that the canonizing function can be computed easily. The same approach was taken by Wale et al. (2008) considering larger connected subgraphs of labeled graphs derived from chemical compounds. On the contrary, for attributed graphs with continuous vertex labels, the function $k_{\simeq}$ is not sufficient to compare subgraphs adequately. Therefore, subgraph matching kernels were proposed by Kriege and Mutzel (2012), which allow to specify arbitrary kernel functions to compare vertex and edge attributes. Essentially, this kernel considers all mappings between subgraphs and scores each mapping by the product of vertex and edge kernel values of the vertex and edge pairs involved in the mapping. When the specified vertex and edge kernels are Dirac kernels, the subgraph matching kernel is equal to the subgraph kernel up to a factor taking the number of automorphisms between subgraphs into account (Kriege and Mutzel, 2012). Based on the above observations explicit mapping of subgraph matching kernels is likely to be more efficient when subgraphs can be adequately compared by a binary kernel.

### 6.2 Weighted Vertex Kernels for Attributed Graphs

Kernels suitable for attributed graphs typically use user-defined kernels for the comparison of vertex and edge annotations like real-valued vectors. The graph kernel is then obtained by combining these kernels according to closure properties. Recently proposed kernels for attributed graphs like GRAPHHOPPER (Feragen et al., 2013) and GRAPHINVARIANT (Orsini et al., 2015) use separate kernels for the graph structure and annotations. They can be expressed as

$$k^{\mathrm{WV}}(G,H) = \sum_{v \in V(G)} \sum_{v' \in V(H)} k_W(v,v') \cdot k_V(v,v'), \tag{7}$$

where $k_V$ is a user-specified kernel comparing vertex attributes and $k_W$ is a kernel that determines a weight for a vertex pair based on the individual graph structures. Hence, in the following we refer to Equation (7) as *weighted vertex kernel*. Kernels belonging to this family are easily identifiable as instances of $R$-convolution kernels, cf. Definition 10.

For graphs with multi-dimensional real-valued vertex annotations in $\mathbb{R}^d$ one could set $k_V$ to the Gaussian RBF kernel $k_{\mathrm{RBF}}$ or the dimension-wise product of the hat kernel $k_\Delta$, respectively, i.e.,

$$k_{\mathrm{RBF}}(x,y) = \exp\left(-\frac{\|x-y\|_2^2}{2\sigma^2}\right) \quad \text{and} \quad k_\Delta(x,y) = \prod_{i=1}^{d} \max\left\{0, 1 - \frac{|x_i - y_i|}{\delta}\right\}. \tag{8}$$

Here, $\sigma$ and $\delta$ are parameters controlling the decrease of the kernel value with increasing discrepancy between the two input data points. The selection of the kernel $k_W$ is essential to take the graph structure into account and allows to obtain different instances of weighted vertex kernels.

### 6.2.1 WEIGHTED VERTEX KERNEL INSTANCES

One approach to obtain weights for pairs of vertices is to compare their neighborhood by the classical Weisfeiler-Lehman label refinement (Shervashidze et al., 2011; Orsini et al., 2015). For a parameter $h$ and a graph $G$ with uniform initial labels $\tau_0$, a sequence $(\tau_1, \ldots, \tau_h)$ of refined labels referred to as *colors* is computed, where $\tau_i$ is obtained from $\tau_{i-1}$ by the following procedure. Sort the multiset of colors $\{\!\{\tau_{i-1}(u) : vu \in E(G)\}\!\}$ for every vertex $v$ to obtain a unique sequence of colors and add $\tau_{i-1}(v)$ as first element. Assign a new color $\tau_i(v)$ to every vertex $v$ by employing an injective mapping from sequences to new colors. A reasonable implementation of $k_W$ motivated along the lines of GRAPHINVARIANT (Orsini et al., 2015) is

$$k_W(v, v') = \sum_{i=0}^{h} k_\delta(\tau_i(v), \tau_i(v')), \tag{9}$$

where $\tau_i(v)$ denotes the discrete label of the vertex $v$ after the $i$-th iteration of Weisfeiler-Lehman label refinement of the underlying unlabeled graph. Intuitively, this kernel reflects to what extent the two vertices have a structurally similar neighborhood.

Another graph kernel, which fits into the framework of weighted vertex kernels, is the GRAPHHOPPER kernel (Feragen et al., 2013) with

$$k_W(v, v') = \langle \mathbf{M}(v), \mathbf{M}(v') \rangle_F \,. \tag{10}$$

Here $\mathbf{M}(v)$ and $\mathbf{M}(v')$ are $\delta \times \delta$ matrices, where the entry $\mathbf{M}(v)_{ij}$ for $v$ in $V(G)$ counts the number of times the vertex $v$ appears as the $i$-th vertex on a shortest path of discrete length $j$ in $G$, where $\delta$ denotes the maximum diameter over all graphs, and $\langle \cdot, \cdot \rangle_F$ is the Frobenius inner product.

### 6.2.2 COMPUTING EXPLICIT FEATURE MAPS

In the following we derive an explicit mapping for weighted vertex kernels. Notice that Equation (7) is an instance of Definition 10. Hence, by Proposition 6 and Equation (4), we obtain an explicit mapping $\phi^{\text{WV}}$ of weighted vertex kernels.

**Proposition 12** *Let $k^{WV}$ be a weighted vertex kernel according to Equation* (7) *with $\phi^W$ and $\phi^V$ feature maps for $k_W$ and $k_V$, respectively. Then*

$$\phi^{WV}(G) = \sum_{v \in V(G)} \phi^W(v) \otimes \phi^V(v) \tag{11}$$

*is a feature map for $k^{WV}$.*

Widely used kernels for the comparison of attributes, such as the Gaussian RBF kernel, do not have feature maps of finite dimension. However, Rahimi and Recht (2008) obtained finite-dimensional feature maps approximating the kernels $k_{\text{RBF}}$ and $k_\Delta$ of Equation (8). Similar results are known for other popular kernels for vectorial data like the Jaccard (Vedaldi and Zisserman, 2012) and the Laplacian kernel (Andoni, 2009).

In the following we approximate $k_V(v, w)$ in Equation (7) by $\langle \widetilde{\phi}^{\text{V}}(v), \widetilde{\phi}^{\text{V}}(w) \rangle$, where $\widetilde{\phi}^{\text{V}}$ is an finite-dimensional, approximative mapping, such that with probability $(1 - \delta)$ for $\delta \in [0, 1]$

$$\sup_{v,w \in V(G)} \left| \left\langle \widetilde{\phi}^{\text{V}}(v), \widetilde{\phi}^{\text{V}}(w) \right\rangle - k_V(v, w) \right| < \varepsilon, \tag{12}$$

for any $\varepsilon > 0$, and derive a finite-dimensional, approximative feature map for weighted vertex kernels. We get the following result.

**Proposition 13** *Let $k^{WV}$ be a weighted vertex kernel. Let $\phi^W$ be a feature map for $k_W$ and let $\widetilde{\phi}^V$ be an approximative mapping for $k_V$ according to Equation* (12)*. Then we can compute an approximative feature map $\widetilde{\phi}^{WV}$ for $k^{WV}$ such that with any constant probability*

$$\sup_{G,H\in\mathcal{G}} \left| \left\langle \widetilde{\phi}^{WV}(G), \widetilde{\phi}^{WV}(H) \right\rangle - k^{WV}(G,H) \right| < \lambda, \tag{13}$$

*for any $\lambda > 0$.*

**Proof** By setting the failure probability to $\delta/|\mathcal{G}|$, and using the union bound we get that for every pair of vertices in the data set with probability $(1-\delta)$

$$\left| \left\langle \widetilde{\phi}^{\mathrm{V}}(v), \widetilde{\phi}^{\mathrm{V}}(w) \right\rangle - k_V(v,w) \right| < \varepsilon\,.$$

The result then follows from Proposition 12, and by setting $\lambda = \varepsilon/(k^{\mathrm{W}}_{\max} \cdot |V_{\max}|^2)$, where $k^{\mathrm{W}}_{\max}$ is the maximum value attained by the kernel $k^{\mathrm{W}}$ and $|V_{\max}|$ is the maximum number of vertices over the whole data set. ■

### 6.3 Explicit and Implicit Computation of Fixed Length Walk Kernels

The classical walk based graph kernels (Gärtner et al., 2003; Kashima et al., 2003), in theory, take all walks without a limitation of length into account. However, in several applications it has been reported that only walks up to a certain length have been considered, e.g., for the prediction of protein functions (Borgwardt et al., 2005) or image classification (Harchaoui and Bach, 2007). This might suggest that it is not necessary or even not beneficial to consider the infinite number of possible walks to obtain a satisfying prediction accuracy. Recently, the phenomenon of *halting* in random walk kernels has been studied (Sugiyama and Borgwardt, 2015), which refers to the fact that walk-based graph kernels like the geometric random walk kernel (Gärtner et al., 2003) might down-weight longer walks so much that their value is dominated by walks of length 1. As a consequence, *fixed length walk kernels*, which consider only walks of (at most) a specified length become promising, in particular for graphs with high degree.

We propose an explicit and implicit computation scheme for fixed length walk kernels. Our product graph based implicit computation scheme fully supports arbitrary vertex and edge kernels and exploits their sparsity. Previously no algorithms based on explicit mapping for computation of walk-based kernels have been proposed. We identify the label diversity and walk lengths as key parameters affecting the running time. This is confirmed experimentally in Section 7.

#### 6.3.1 BASIC DEFINITIONS

A fixed length walk kernel measures the similarity between graphs based on the similarity between all pairs of walks of length $\ell$ contained in the two graphs. A walk of length $\ell$ in a graph $G$ is a sequence of vertices and edges $(v_0, e_1, v_1, \ldots, e_\ell, v_\ell)$ such that $e_i = v_{i-1}v_i \in E(G)$ for $i \in \{1, \ldots, \ell\}$. We denote the set of walks of length $\ell$ in a graph $G$ by $\mathcal{W}_\ell(G)$.

**Definition 14 ($\ell$-walk kernel)** *The* $\ell$-walk kernel *between two attributed graphs* $G$ *and* $H$ *in* $\mathcal{G}$ *is defined as*

$$K_\ell^=(G,H) = \sum_{w \in \mathcal{W}_\ell(G)} \sum_{w' \in \mathcal{W}_\ell(H)} k_W(w,w'), \tag{14}$$

*where* $k_W$ *is a kernel between walks.*

Definition 14 is very general and does not specify how to compare walks. An obvious choice is to decompose walks and define $k_W$ in terms of vertex and edge kernel functions, denoted by $k_V$ and $k_E$, respectively. We consider

$$k_W(w,w') = \prod_{i=0}^{\ell} k_V(v_i,v_i') \prod_{i=1}^{\ell} k_E(e_i,e_i'), \tag{15}$$

where $w = (v_0, e_1, \ldots, v_\ell)$ and $w' = (v_0', e_1', \ldots, v_\ell')$ are two walks.[2] Assume the graphs in a data set have simple vertex and edge labels $\tau : V \uplus E \to \mathcal{L}$. An appropriate choice then is to use the Dirac kernel for both, vertex and edge kernels, between the associated labels. In this case two walks are considered equal if and only if the labels of all corresponding vertices and edges are equal. We refer to this kernel by

$$k_W^\delta(w,w') = \prod_{i=0}^{\ell} k_\delta(\tau(v_i),\tau(v_i')) \prod_{i=1}^{\ell} k_\delta(\tau(e_i),\tau(e_i')), \tag{16}$$

where $k_\delta$ is the Dirac kernel. For graphs with continuous or multi-dimensional annotations this choice is not appropriate and $k_V$ and $k_E$ should be selected depending on the application-specific vertex and edge attributes.

A variant of the $\ell$-walk kernel can be obtained by considering all walks up to length $\ell$.

**Definition 15 (Max-$\ell$-walk kernel)** *The* Max-$\ell$-walk kernel *between two attributed graphs* $G$ *and* $H$ *in* $\mathcal{G}$ *is defined as*

$$K_\ell^\leq(G,H) = \sum_{i=0}^{\ell} \lambda_i K_i^=(G,H), \tag{17}$$

*where* $\lambda_0, \ldots, \lambda_\ell \in \mathbb{R}_{\geq 0}$ *are weights.*

In the following we primary focus on the $\ell$-walk kernel, although our algorithms and results can be easily transferred to the Max-$\ell$-walk kernel.

### 6.3.2 WALK AND $R$-CONVOLUTION KERNELS

We show that the $\ell$-walk kernel is p.s.d. if $k_W$ is a valid kernel by seeing it as an instance of an $R$-convolution kernel. We use this fact to develop an algorithm for explicit mapping based on the ideas presented in Section 5.4.

**Proposition 16** *The* $\ell$*-walk kernel is positive semidefinite if* $k_W$ *is defined according to Equation* (15) *and* $k_V$ *and* $k_E$ *are valid kernels.*

2. The same idea to compare walks was proposed by Kashima et al. (2003) as part of the marginalized kernel between labeled graphs.

**Proof** Equation (14) with $k_W$ defined according to Equation (15) is the $R$-convolution kernel, cf. Definition 10, directly obtained when graphs are decomposed into walks $w = (v_0, e_1, v_1, \ldots, e_\ell, v_\ell) = (x_0, \ldots, x_{2\ell})$ and

$$k_i = \begin{cases} k_V & \text{if } i \text{ even,} \\ k_E & \text{otherwise} \end{cases}$$

for $i \in \{0, \ldots, 2\ell\}$. Then $k_W$ equals $\prod_{i=0}^{2\ell} k_i(x_i, x_i')$, implying that the $\ell$-walk kernel is a valid kernel if $k_V$ and $k_E$ are valid kernels. ■

Since kernels are closed under taking linear combinations with non-negative coefficients, see Proposition 6, we obtain the following corollary.

**Corollary 17** *The Max-$\ell$-walk kernel is positive semidefinite.*

Since $\ell$-walk kernels are $R$-convolution kernels, we can derive a feature map. Our theoretical results show that the dimension of the feature space and the density of feature vectors for $k_W$ depend multiplicative on the same properties of the feature vectors for $k_V$ and $k_E$. Hence we consider a special case of high practical relevance: We assume graphs to have simple labels from the alphabet $\mathcal{L}$ and consider the kernel $k_W^\delta$ given by Equation (16). A walk $w$ of length $\ell$ is then associated with a label sequence $\tau(w) = (\tau(v_0), \tau(e_1), \ldots, \tau(v_\ell)) \in \mathcal{L}^{2\ell+1}$. In this case graphs are decomposed into walks and two walks $w$ and $w'$ are considered equivalent if and only if $\tau(w) = \tau(w')$; each label sequence can be considered an identifier of an equivalence class of $\sim_{k_W^\delta}$. This gives rise to the feature map $\phi_\ell^=$, where each component is associated with a label sequence $s \in \mathcal{L}^{2\ell+1}$ and counts the number of walks $w \in \mathcal{W}_\ell(G)$ with $\tau(w) = s$. Note that the obtained feature vectors have $|\mathcal{L}|^{2\ell+1}$ components, but are typically sparse.

We can easily derive a feature map of the Max-$\ell$-walk kernel from the feature maps of all $i$-walk kernels with $i \leq \ell$, cf. Proposition 6.

### 6.3.3 IMPLICIT KERNEL COMPUTATION

An essential part of the implicit computation scheme is the generation of the product graph that is then used to compute the $\ell$-walk kernel.

**Computing Direct Product Graphs.** In order to support graphs with arbitrary attributes, vertex and edge kernels $k_V$ and $k_E$ are considered as part of the input. Product graphs can be used to represent these kernel values between pairs of vertices and edges of the input graphs in a compact manner. We avoid to create vertices and edges that would represent incompatible pairs with kernel value zero. The following definition can be considered a weighted version of the direct product graph introduced by Gärtner et al. (2003) for kernel computation.[3]

**Definition 18 (Weighted Direct Product Graph)** *For two attributed graphs $G = (V, E)$, $H = (V', E')$ and given vertex and edge kernels $k_V$ and $k_E$, the* weighted direct product graph *(WDPG)*

3. Note that we consider undirected graphs while Gärtner et al. (2003) refers to directed graphs.

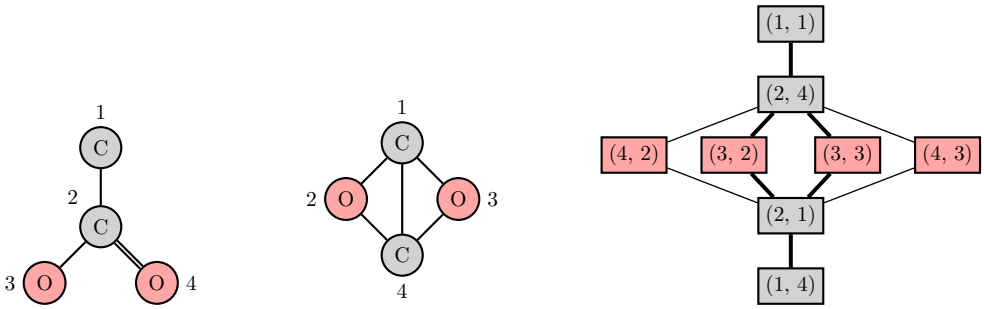


(a) $G$ (b) $H$ (c) $G \times_w H$

Figure 1: Two attributed graphs $G$ (a) and $H$ (b) and their weighted direct product graph $G \times_w H$ (c). We assume the vertex kernel to be the Dirac kernel and $k_E$ to be 1 if edge labels are equal and $\frac{1}{2}$ if one edge label is "=" and the other is "–". Thin edges in $G \times_w H$ represent edges with weight $\frac{1}{2}$, while all other edges and vertices have weight 1.

*is denoted by* $G \times_w H = (\mathcal{V}, \mathcal{E}, w)$ *and defined as*

$$\begin{aligned}
\mathcal{V} &= \big\{(v, v') \in V \times V' \;\big|\; k_V(v, v') > 0\big\} \\
\mathcal{E} &= \big\{(u, u')(v, v') \in [\mathcal{V}]^2 \;\big|\; uv \in E \wedge u'v' \in E' \wedge k_E(uv, u'v') > 0\big\} \\
w(v) &= k_V(u, u') && \forall v = (u, u') \in \mathcal{V} \\
w(e) &= k_E(uv, u'v') && \forall e \in \mathcal{E}, \textit{where } e = (u, u')(v, v').
\end{aligned}$$

An example with two graphs and their weighted direct product graph obtained for specific vertex and edge kernels is shown in Figure 1. Algorithm 3 computes a weighted direct product graph and does not consider edges between pairs of vertices $(v, v')$ that have been identified as incompatible, i.e., $k_V(v, v') = 0$.

Since the weighted direct product graph is undirected, we must avoid that the same pair of edges is processed twice. Therefore, we suppose that there is an arbitrary total order $\prec$ on the vertices $\mathcal{V}$, such that for every pair $(u, s), (v, t) \in \mathcal{V}$ either $(u, s) \prec (v, t)$ or $(v, t) \prec (u, s)$ holds. In line 8 we restrict the edge pairs that are compared to one of these cases.

**Proposition 19** *Let* $n = |V(G)|$, $n' = |V(H)|$ *and* $m = |E(G)|$, $m' = |E(H)|$. *Algorithm 3 computes the weighted direct product graph in time* $\mathcal{O}(nn'\mathsf{T}_V + mm'\mathsf{T}_E)$, *where* $\mathsf{T}_V$ *and* $\mathsf{T}_E$ *is the running time to compute vertex and edge kernels, respectively.*

Note that in case of a sparse vertex kernel, which yields zero for most of the vertex pairs of the input graph, $|V(G \times_w H)| \ll |V(G)| \cdot |V(H)|$ holds. Algorithm 3 compares two edges by $k_E$ only in case of matching endpoints (cf. lines 7, 8), therefore in practice the running time to compare edges (line 7–13) might be considerably less than suggested by Proposition 19. We show this empirically in Section 7.3. In case of sparse graphs, i.e., $|E| = \mathcal{O}(|V|)$, and vertex and edge kernels which can be computed in time $\mathcal{O}(1)$ the running time of Algorithm 3 is $\mathcal{O}(n^2)$, where $n = \max\{|V(G)|, |V(H)|\}$.

**Algorithm 3:** Weighted Direct Product Graph

**Input** : Graphs $G$ and $H$, vertex and edge kernels $k_V$ and $k_E$.
**Output** : Graph $G \times_w H = (\mathcal{V}, \mathcal{E}, w)$.

**Procedure** WDPG($G, H, k_V, k_E$)

**forall** $v \in V(G)$, $v' \in V(H)$ **do**
  $w \leftarrow k_V(v, v')$
  **if** $w > 0$ **then**
    create vertex $z = (v, v')$
    $\mathcal{V} \leftarrow \mathcal{V} \uplus \{z\}$
    $w(z) = w$
**forall** $(u, s) \in \mathcal{V}$ **do**
  **forall** $v \in \mathrm{N}(u), t \in \mathrm{N}(s)$ *with* $(v, t) \in \mathcal{V}$, $(u, s) \prec (v, t)$ **do**
    $w \leftarrow k_E(uv, st)$
    **if** $w > 0$ **then**
      create edge $e = (u, s)(v, t)$
      $\mathcal{E} \leftarrow \mathcal{E} \uplus \{e\}$
      $w(e) = w$

**Counting Weighted Walks.** Given an undirected graph $G$ with adjacency matrix $\mathbf{A}$, let $a_{ij}^\ell$ denote the element at $(i, j)$ of the matrix $\mathbf{A}^\ell$. It is well-known that $a_{ij}^\ell$ is the number of walks from vertex $i$ to $j$ of length $\ell$. The number of $\ell$-walks of $G$ consequently is $\sum_{i,j} a_{i,j}^\ell = \mathbf{1}^\top \mathbf{A}^\ell \mathbf{1} = \mathbf{1}^\top \mathbf{r}_\ell$, where $\mathbf{r}_\ell = \mathbf{A}\mathbf{r}_{\ell-1}$ with $\mathbf{r}_0 = \mathbf{1}$. The $i$-th element of the recursively defined vector $\mathbf{r}_\ell$ is the number of walks of length $\ell$ starting at vertex $i$. Hence, we can compute the number of $\ell$-walks by computing either matrix powers or matrix-vector products. Note that even for sparse (connected) graphs $\mathbf{A}^\ell$ quickly becomes dense with increasing walk length $\ell$. The $\ell$-th power of an $n \times n$ matrix $\mathbf{A}$ can be computed naïvely in time $\mathcal{O}(n^\omega \ell)$ and $\mathcal{O}(n^\omega \log \ell)$ using exponentiation by squaring, where $\omega$ is the exponent of matrix multiplication. The vector $\mathbf{r}_\ell$ can be computed by means of matrix-vector multiplications, where the matrix $\mathbf{A}$ remains unchanged over all iterations. Since direct product graphs tend to be sparse in practice, we propose a method to compute the $\ell$-walk kernel that is inspired by matrix-vector multiplication.

In order to compute the $\ell$-walk kernel we do not want to count the walks, but sum up the weights of each walk, which in turn are the product of vertex and edge weights. Let $k_W$ be defined according to Equation (15), then we can formulate the $\ell$-walk kernel as

$$K_\ell^=(G, H) = \sum_{w \in \mathcal{W}_\ell(G)} \sum_{w' \in \mathcal{W}_\ell(H)} k_W(w, w') = \sum_{v \in V(G \times_w H)} r_\ell(v), \tag{18}$$

where $r_\ell$ is determined recursively according to

$$\begin{aligned} r_i(u) &= \sum_{uv \in E(G \times_w H)} w(u) \cdot w(uv) \cdot r_{i-1}(v) && \forall u \in V(G \times_w H) \\ r_0(u) &= w(u) && \forall u \in V(G \times_w H). \end{aligned}$$

Note that $r_i$ can as well be formulated as matrix-vector product. We present a graph-based approach for computation akin to sparse matrix-vector multiplication, see Algorithm 4.

**Algorithm 4:** Implicit computation of $\ell$-walk kernel

**Input** : Graphs $G$, $H$, kernels $k_V$, $k_E$ and length parameter $\ell$.
**Output** : Value $K_\ell^=(G,H)$ of the $\ell$-walk kernel.

```
1 (V, E, w) ← WDPG(G, H, k_V, k_E)                    ▷ Compute G ×_w H
2 forall v ∈ V do
3     r_0(v) ← w(v)                                    ▷ Initialization
4 for i ← 1 to ℓ do
5     forall u ∈ V do
6         r_i(u) ← 0
7         forall v ∈ N(u) do                           ▷ Neighbors of u in G ×_w H
8             r_i(u) ← r_i(u) + w(u) · w(uv) · r_{i−1}(v)
9 return Σ_{v∈V} r_ℓ(v)
```

**Theorem 20** *Let $n = |\mathcal{V}|$, $m = |\mathcal{E}|$. Algorithm 4 computes the $\ell$-walk kernel in time $\mathcal{O}(n + \ell(n + m) + \mathsf{T}_{\text{WDPG}})$, where $\mathsf{T}_{\text{WDPG}}$ is the time to compute the weighted direct product graph.*

Note that the running time depends on the size of the product graph and $n \ll |V(G)| \cdot |V(H)|$ and $m \ll |E(G)| \cdot |E(H)|$ is possible as discussed in Section 6.3.3.

The Max-$\ell$-walk kernel is the sum of the $j$-walk kernels with $j \leq \ell$ and, hence, with Equation (18) we can also formulate it recursively as

$$K_\ell^\leq(G,H) = \sum_{i=0}^{\ell} \lambda_i K_i^=(G,H) = \sum_{i=0}^{\ell} \lambda_i \sum_{v \in V(G \times_w H)} r_i(v). \tag{19}$$

This value can be obtained from Algorithm 4 by simply changing the return statement in line 9 according to the right-hand side of the equation without affecting the asymptotic running time.

### 6.3.4 EXPLICIT KERNEL COMPUTATION

Provided that we have an explicit feature map for the kernel $k_V$ and $k_E$ on walks, we obtain an explicit computation schemes by enumerating all walks and combining their feature maps, cf. Section 5. We again consider graphs with simple labels from the alphabet $\mathcal{L}$ and the kernel $k_W^\delta$ given by Equation (16). We develop an efficient algorithm tailored to this setting, which computes the feature vectors described in Section 6.3.2.

Instead of enumerating all walks in order to count their label sequences, we propose a more elaborated approach that exploits the simple composition of walks similar to the approach for weighted walks, cf. Section 6.3.3. A walk of length $\ell$ can be decomposed into a walk of length $\ell - 1$ with an additional edge and vertex added at the front. This allows to obtain the number of walks of length $\ell$ with a given label sequence starting at a fixed vertex $v$ by concatenating $(\tau(v), \tau(vu))$ with all label sequences for walks starting from a neighbor $u$ of the vertex $v$. Algorithm 5 provides the pseudo code of this computation.

**Algorithm 5:** Generating feature vectors of the $\ell$-walk kernel

**Input** : Graph $G$, length parameter $\ell$.
**Output** : Feature vector $\phi_\ell^=(G)$ of label sequences and counts associated with length $\ell$ walks in $G$.
**Data** : Feature vectors $\Phi_i^v : \mathcal{L}^{2i+1} \to \mathbb{N}$ of label sequences associated with $i$-walks starting at $v$.

```
forall v ∈ V(G) do
    Φ_0^v(τ(v)) ← 1                                  ▷ Initialization, length 0 walks
for i ← 1 to ℓ do
    forall u ∈ V(G) and v ∈ N(u) do
        forall w with Φ_{i-1}^v(w) > 0 do
            w' ← (τ(u), τ(uv)) + w                   ▷ Concatenate label sequence
            Φ_i^u(w') ← Φ_i^u(w') + Φ_{i-1}^v(w)
return Σ_{v∈V(G)} Φ_ℓ^v                              ▷ Combine vectors
```

**Theorem 21** *Given a graph $G$ with $n = |V(G)|$ vertices and $m = |E(G)|$ edges, Algorithm 5 computes the $\ell$-walk kernel feature vector $\phi_\ell^=(G)$ in time $\mathcal{O}(n+\ell(n+m)s)$, where $s$ is the maximum number of different label sequences of $(\ell-1)$-walks staring at a vertex of $G$.*

Assume Algorithm 5 is applied to unlabeled sparse graphs, i.e., $|E(G)| = \mathcal{O}(|V(G)|)$, then $s = 1$ and the feature mapping can be performed in time $\mathcal{O}(n + \ell n)$. With Proposition 2 we have a total running time to compute a kernel matrix for $d$ graphs of order $n$ of $\mathcal{O}(d\ell n + d^2)$, for $\ell > 0$.

### 6.4 Discussion

In this section we have studied the implicit and explicit computation of several graph kernels, the basic characteristics are summarized in Table 2. The practicability of explicit computation crucially depends on the dimension of the feature space associated with the base vertex and edge kernels. This dependence is essential for the shortest path kernel and, in particular, for the fixed length walk kernel and the subgraph matching kernel. When sparse data structures are employed, the sparsity of the feature vectors of the vertex and edge kernels becomes an important intervening factor, which is difficult to assess theoretically. Considering the relevant special case of a Dirac kernel, which leads to feature vectors with only one non-zero component, the rapid growth due to multiplication is tamed. In this case the number of substructures considered as different according to the vertex and edge kernels determines the number of non-zero components of the feature vectors associated with the graph kernel.

## 7. Experimental Evaluation

To obtain authoritative experimental results we carefully implemented and engineered algorithms for both, implicit and explicit, computation.

Table 2: Graph kernels and their properties. We consider graphs on $n$ vertices and $m$ edges with maximum degree $\Delta$. Let $\delta$ be the maximum diameter of any graph $G$ in the data sets and $C$ the total number of colors appearing in $h$ iterations of Weisfeiler-Lehman refinement. The dimension of the feature space associated with $k_V$ and $k_E$ is denoted by $d_V$ and $d_E$, respectively, while $\mathsf{T}_V$ and $\mathsf{T}_E$ is the time to evaluate the vertex and edge kernel once. The parameters $\ell$ and $k$ denote the walk length and subgraph size, respectively.

| **Graph kernel** | **Parts** | **Dimension** | **Running time IM** |
|---|---|---|---|
| SHORTESTPATH | $\mathcal{O}(n^2)$ | $d_V^2 d_E$ | $\mathcal{O}\left(n^2\mathsf{T}_V + n^4\mathsf{T}_E\right)$ |
| GRAPHHOPPER | $\mathcal{O}(n)$ | $\delta^2 d_V$ | $\mathcal{O}\left(n^2(m + \log n + \mathsf{T}_V + \delta^2)\right)$ |
| GRAPHINVARIANT | $\mathcal{O}(n)$ | $Cd_V$ | $\mathcal{O}\left(hm + n^2\mathsf{T}_V\right)$ |
| FIXEDLENGTHRANDOMWALK | $\mathcal{O}(\Delta^\ell)$ | $d_V + (d_V d_E)^\ell$ | $\mathcal{O}\left(\ell(n^2 + m^2) + n^2\mathsf{T}_V + m^2\mathsf{T}_E\right)$ |
| SUBGRAPHMATCHING | $\mathcal{O}(n^k)$ | $(d_V d_E^2)^k k!$ | $\mathcal{O}\left(kn^{2k+2} + n^2\mathsf{T}_V + n^4\mathsf{T}_E\right)$ |

### 7.1 Experimental Setup

All algorithms were implemented in Java and the default Java `HashMap` class was used to store feature vectors, see Section 4.2. Due to the varied memory requirements of individual series of experiments, different hardware platforms were used in Sections 7.2, 7.3 and 7.4. Unless stated otherwise the reported running times refer to the computation of the quadratic kernel matrices. We performed classification experiments using the $C$-SVM implementation LIBSVM (Chang and Lin, 2011). We report mean prediction accuracies obtained by 10-fold cross-validation repeated 10 times with random fold assignments. Within each fold all necessary parameters were selected by cross-validation based on the training set. This includes the regularization parameter $C$ selected from $\{10^{-3}, 10^{-2}, \ldots, 10^3\}$, all kernel parameters, where applicable, and whether to normalize the kernel matrix.

#### 7.1.1 DATA SETS

We performed experiments on synthetic and real-world data sets from different domains, see Table 3 for an overview on their characteristics. All data sets can be obtained from our publicly available collection (Kersting et al., 2016) unless the source is explicitly stated below.

**Small Molecules.** Molecules can naturally be represented by graphs, where vertices represent atoms and edges represent chemical bonds. MUTAG is a data set of chemical compounds divided into two classes according to their mutagenic effect on a bacterium. This small data set is commonly used in the graph kernel literature. In addition we considered the larger data set U251, which stems from the NCI Open Database provided by the National Cancer Institute (NCI). In this data set the class labels indicate the ability of a compound to inhibit the growth of the tumor cell line U251. We used the data set processed by Swamidass et al. (2005), which is publicly available from the ChemDB website.[4]

**Macromolecules.** ENZYMES and PROTEINS both represent macromolecular structures and were obtained from (Borgwardt et al., 2005; Feragen et al., 2013). The following graph model has been

4. `http://cdb.ics.uci.edu`

Table 3: Data set statistics and properties.

| Data set | Properties | | | | | |
|---|---|---|---|---|---|---|
| | Graphs | Classes | Avg. $\lvert V\rvert$ | Avg. $\lvert E\rvert$ | Vertex/edge labels | Attributes |
| MUTAG | 188 | 2 | 17.9 | 19.8 | +/+ | − |
| U251 | 3 755 | 2 | 23.1 | 24.8 | +/+ | − |
| ENZYMES | 600 | 6 | 32.6 | 62.1 | +/+ | 18 |
| PROTEINS | 1 113 | 2 | 39.1 | 72.8 | +/− | 1 |
| SYNTHETICNEW | 300 | 2 | 100.0 | 196.3 | −/− | 1 |
| SYNTHIE | 400 | 4 | 95.0 | 172.9 | −/− | 15 |

employed. Vertices represent secondary structure elements (SSE) and are annotated by their type, i.e., helix, sheet or turn, and a rich set of physical and chemical attributes. Two vertices are connected by an edge if they are neighbors along the amino acid sequence or one of three nearest neighbors in space. Edges are annotated with their type, i.e., structural or sequential. In ENZYMES each graph is annotated by an EC top level class, which reflects the chemical reaction the enzyme catalyzes, PROTEINS is divided into enzymes and non-enzymes.

**Synthetic Graphs.** The data sets SYNTHETICNEW and SYNTHIE were synthetically generated to obtain classification benchmarks for graph kernels with attributes. We refer the reader to the publications (Feragen et al., 2013)[5] and (Morris et al., 2016), respectively, for the details of the generation process. Additionally, we generated new synthetic graphs in order to systematically vary graph properties of interest like the label diversity, which we expect to have an effect on the running time according to our theoretical analysis.

### 7.2 Implicit and Explicit Computation of Kernels for Attributed Graphs

We have derived explicit computation schemes of kernels for attributed graphs, which have been proposed with an implicit method of computation. Approximative explicit computation is possible under the assumption that the kernel for the attributes can be approximated by explicit feature maps. We compare both methods of computation w.r.t. their running time and the obtained classification accuracy on the four attributed graph data sets ENZYMES, PROTEINS, SYNTHETICNEW and SYNTHIE. Since the discrete labels alone are often highly informative, we ignored discrete labels if present and considered the real-valued vertex annotations only in order to obtain challenging classification problems. All attributes where dimension-wise linearly scaled to the range $[0..1]$ in a preprocessing step.

We employed three kernels for attributed graphs: the shortest-path kernel, cf. Section 6.1.1, and the GRAPHHOPPER and GRAPHINVARIANT kernel as described in Section 6.2.1. We used the Dirac kernel to compare shortest-path lengths and selected the number of Weisfeiler-Lehman refinement steps for the GRAPHINVARIANT kernel from $h \in \{0, \ldots, 7\}$. For the comparison of attributes we employed the dimension-wise product of hat kernel $k_{\Delta}$ as defined in Equation (8) choosing $\delta$ from $\{0.2, 0.4, 0.6, 0.8, 1.0, 1.5, 2.0\}$. The three kernels were computed functionally employing this

5. We used the updated version of the data set SYNTHETIC published together with the Erratum to (Feragen et al., 2013).

kernel as a base line. We obtained approximate explicit feature maps for the attribute kernel by the method of Rahimi and Recht (2008) and used these to derive approximate explicit feature maps for the graph kernels. We varied the number of non-zero components of the feature vectors for the attribute kernel, i.e., the number of random binning features, from $\{1, 2, 4, 8, 16, 32, 64\}$. Please note that the running time is effected by the kernel parameters, i.e., $\delta$ of Equation (8) and the number $h$ of Weisfeiler-Lehman refinement steps for GRAPHINVARIANT. Therefore, in the following we report the running times for fixed values $\delta = 1$ and $h = 3$, which were selected frequently by cross-validation. All experiments were conducted using Oracle Java v1.8.0 on an Intel Xeon E5-2640 CPU at 2.5GHz with 64GB of RAM using a single processor only.

#### 7.2.1 RESULTS AND DISCUSSION

We were not able to compute the shortest-path kernel by explicit feature maps with more than 16 iterations of binning for the base kernel on ENZYMES and PROTEINS and no more than 4 iterations on SYNTHIE and SYNTHETICNEW with 64 GB of main memory. The high memory consumption of this kernel is in accordance with our theoretical analysis, since the multiplication of vertex and edge kernels drastically increases the number of non-zero components of the feature vectors. This problem does not effect the two weighted vertex kernels to the same extent. We observed the general trend that the memory consumption and running time increases with small values of $\delta$. This is explained by the fact that the number of components of the feature vectors of the vertex kernels increases in this case. Although the number of non-zero components does not increase for these feature vectors, it does for the graph kernel feature vectors, since the number of vertices with attributes falling into different bins increases.

The results on running time and accuracy are summarized in Figure 2. For the two data sets ENZYMES and SYNTHIE we observe that the classification accuracy obtained by the approximate explicit feature maps approaches the accuracy obtained by the exact method with increasing number of binning iterations. For the other two data sets the number of iterations has no distinct effect on the prediction accuracy. Even the kernels obtained with a single iteration of binning, i.e., essentially applying a Dirac kernel, achieves the same accuracy as the exact kernel obtained by implicit computation. This suggests that a trivial comparison of attributes is sufficient for these data sets or that attributes are not essential for classification at all.

With few iteration of binning the explicit computation scheme is always faster than the implicit computation. The growth in running time with increasing number of binning iterations for the vertex kernel varies between the graph kernels. Approximating the GRAPHHOPPER kernel by explicit feature maps with 64 binning iteration for the vertex kernel leads to a running time similar to the one required for its exact implicit computation on all data sets with exception of SYNTHETICNEW. On this data set explicit computation remains faster. For GRAPHINVARIANT explicit feature maps lead to a running time which is orders of magnitude lower than implicit computation. Although both, GRAPHHOPPER and GRAPHINVARIANT are weighted vertex kernels, this difference can be explained by the number of non-zero components in the feature vectors of the weight kernel. We observe that GRAPHINVARIANT clearly provides the best classification accuracy for two of the four data sets and is competitive for the other two. At the same time GRAPHINVARIANT can be approximated very efficiently by explicit feature maps. Therefore, even for attributed graphs effective and efficient graph kernels can be obtained from explicit feature maps by our approach.

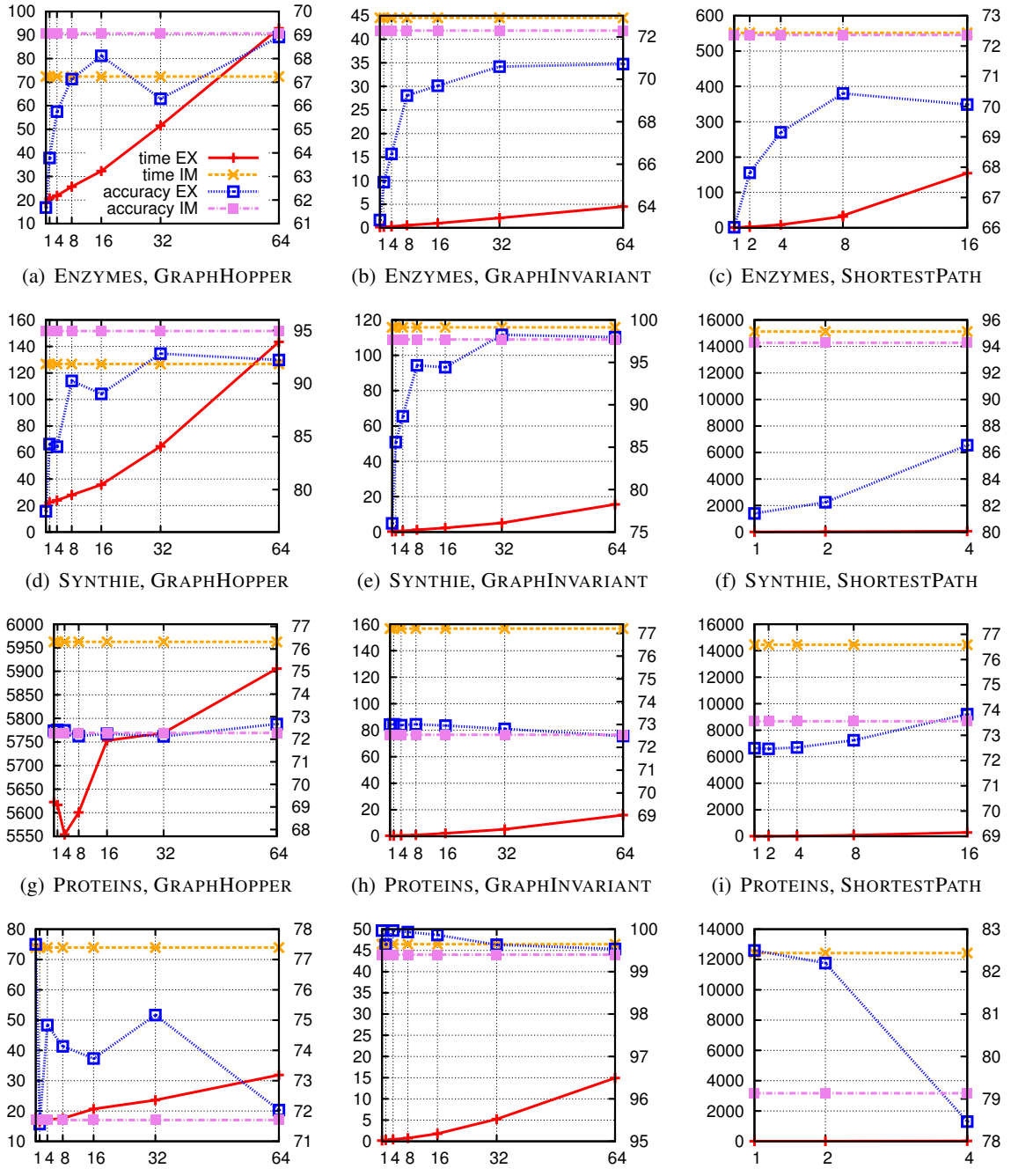


(a) ENZYMES, GRAPHHOPPER (b) ENZYMES, GRAPHINVARIANT (c) ENZYMES, SHORTESTPATH

(d) SYNTHIE, GRAPHHOPPER (e) SYNTHIE, GRAPHINVARIANT (f) SYNTHIE, SHORTESTPATH

(g) PROTEINS, GRAPHHOPPER (h) PROTEINS, GRAPHINVARIANT (i) PROTEINS, SHORTESTPATH

(j) SYNTHETICNEW, GRAPHHOPPER (k) SYNTHETICNEW, GRAPHINVARIANT (l) SYNTHETICNEW, SHORTESTPATH

Figure 2: Running times and classification accuracies of graph kernels approximated by explicit feature maps with $2^i$, $i \in \{0, \ldots, 4\}$, iterations of random binning. The results of exact implicit computation are shown as a base line (left $y$-axes shows the running time in seconds, right $y$-axes the accuracy in percent).

### 7.3 Implicit and Explicit Computation of Walk Kernels for Graphs with Discrete Labels

Our comparison in the previous section showed that computation by explicit feature maps becomes prohibitive when vertex and edge kernels with feature vectors having multiple non-zero components are multiplied. This is observed for the shortest-path kernel, which applies a walk kernel of fixed length one. Therefore, we study the implicit and explicit computation schemes of the fixed length walk kernel on graphs with discrete labels, which are compared by the Dirac kernel, cf. Equation (16). Since both computation schemes produced the same kernel matrices, our main focus in this section is on running times.

The discussion of running times for walk kernels in Sections 6.3.3 and 6.3.4 suggested that

(i) implicit computation benefits from sparse vertex and edge kernels,
(ii) explicit computation is promising for graphs with a uniform label structure, which exhibit few different features, and then scales to large data sets.

We experimentally analyze this trade-off between label diversity and running time for synthetic and real-world data sets. Finally, we use our walk kernels to compare graphs after applying different levels of label refinement using the Weisfeiler-Lehman method and to compute the shortest-path kernel on graphs with discrete labels. The experiments reported in this section were conducted using Java OpenJDK v1.7.0 on an Intel Core i7-3770 CPU at 3.4GHz (Turbo Boost disabled) with 16GB of RAM using a single processor only. The reported running times are average values over $5$ runs.

#### 7.3.1 SYNTHETIC DATA SETS

In order to systematically vary the label diversity we generated synthetic graphs by the following procedure: The number of vertices was determined by a Poisson distribution with mean $20$. Edges were inserted between a pair of vertices with probability $0.1$. The label diversity depends on the parameter $p_V$. Edges were uniformly labeled; a vertex obtained the label $0$ with probability $1 - p_V$. Otherwise the labels $1$ or $2$ were assigned with equal probability. In addition, we vary the data set size $d$ between $100$ and $300$ adding $20$ randomly generated graphs in each step.

The results are depicted in Figure 3, where a label diversity of $50$ means that $p_V = 0.5$. Figure 3(a) shows that the running time for implicit computation increases with the data set size and decreases with the label diversity. This observation is in accordance with our hypotheses. When the label diversity increases, there are less compatible pairs of vertices and the weighted direct product graph becomes smaller. Consequently, its computation and the counting of weighted walks require less running time. For explicit computation we observe a different trend: While the running time increases with the size of the data set, the approach is extremely efficient for graphs with uniform labels ($p_V = 0$) and becomes slower when the label diversity increases, cf. Figure 3(b). Combining both results, cf. Figure 3(c), shows that both approaches yield the same running time for a label diversity of $p_V \approx 0.3$, while for higher values of $p_V$ implicit computation is preferable and explicit otherwise.

#### 7.3.2 MOLECULAR DATA SETS

In the previous section we have observed how both approaches behave when the label diversity is varied. We use the data set U251 of graphs derived from small molecules to analyze the running time on a real-world data set with a predetermined label diversity. Vertex labels correspond to the atom types and edge labels represent single, double, triple and aromatic bonds, respectively. This time we

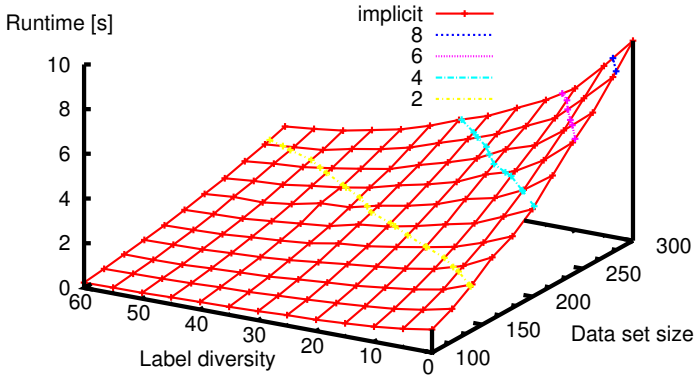


(a) Implicit computation

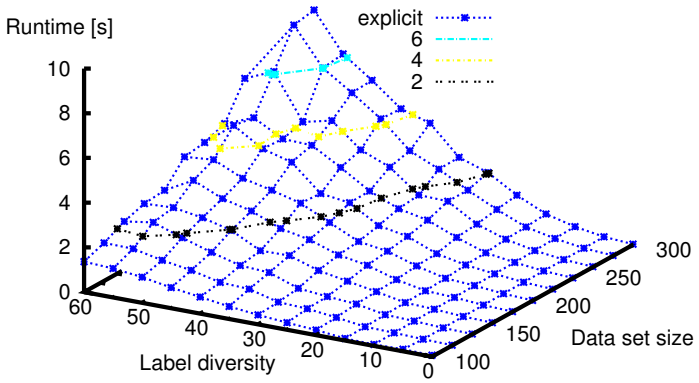


(b) Explicit computation

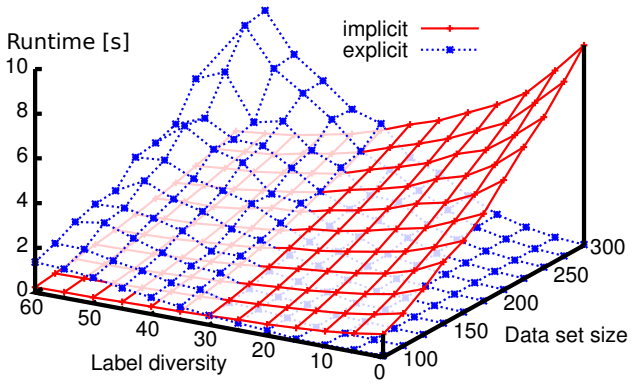


(c) Implicit and explicit computation

Figure 3: Running time to generate the kernel matrix by implicit and explicit computation of walk kernels with fixed length 7 for synthetic data sets with varying label diversity. Figures (a) and (b) show contour lines obtained by linear interpolation.

vary the walk length and the data set size by starting with a random subset and adding additional graphs that were selected randomly from the remaining graphs of the data set.

Figure 4(a) shows that the running time of the implicit computation scheme heavily depends on the size of the data set. The increase with the walk length is less considerable. This can be explained by the time $\mathsf{T}_{\text{WDPG}}$ required to compute the product graph, which is always needed independent of the walk length. For short walks explicit computation is very efficient, even for larger data sets, cf. Figure 4(b). However, when a certain walk length is reached the running time increases drastically. This can be explained by the growing number of different label sequences. Notably for walks of length $8$ and $9$ the running time also largely increases with the data set size. This indicates that the time $\mathsf{T}_{dot}$ has a considerable influence on the running time. In the following section we analyze the running time of the different procedures for the two algorithms in more detail. Figure 4(c) shows that for walk length up to 7 explicit computation beats implicit computation on the molecular data set.

### 7.3.3 ENZYMES AND MUTAG

We have shown that up to a certain walk length explicit computation is more efficient than implicit computation. We want to clarify the relation between the walk length and the prediction accuracy in a classification task. In addition, we analyze the ratio between the time $\mathsf{T}_{\phi}$ for computing the explicit mapping and $\mathsf{T}_{dot}$ for taking dot products. For the implicit computation scheme we want to clarify the running time of $\mathsf{T}_{\text{WDPG}}$ and the time required for counting weighted walks. We apply both algorithms to two widely used data sets, MUTAG and ENZYMES, and vary the walk length, see Table 3 for details on these data sets.

Figure 5 shows the running time of both algorithms depending on the walk length and gives the time for product graph computation and explicit mapping, respectively. In addition, the prediction accuracy is presented. For both data sets we observe that up to a walk length of 7 explicit mapping is more efficient. Notably a peak of the accuracy is reached for walk length smaller than 7 in both cases. For the MUTAG data set walks of length $3$ provide the best results and walks of length $6$ for the ENZYMES data set, i.e., in both cases explicit mapping should be preferred when computing a walk kernel of fixed length. The running time of the product graph computation is constant and does not depend on the walk length. For explicit mapping the time required to compute the dot product becomes dominating when the walk length is increased. This can be explained by the fact that the generation of the kernel matrix involves a quadratic number of dot product computations, see Proposition 2. Note that the given times include a quadratic number of product graph computations while the times for generating the feature vectors include only a linear number of operations.

As a side note, we also compared the accuracy of our kernels based on walks of fixed length to the accuracy reached by the geometric random walk kernel (GRW) according to Gärtner et al. (2003), which considers arbitrary walk lengths. The parameter $\gamma$ of the geometric random walk kernel was selected by cross-validation from $\{10^{-5}, 10^{-4}, \ldots, 10^{-2}\}$. We observed that the accuracy of our kernel is competitive on the MUTAG data set (GRW $87.3$), and considerably better on the ENZYMES data set (GRW $31.6$), cf. Figure 5. This is remarkable, since our approach with walk length $6$ yields best results and is efficiently computed by explicit mapping, which would be impossible for the geometric random walk kernel. For a more detailed discussion and comparison between fixed length walk kernels and the geometric random walk kernel we refer the reader to (Sugiyama and Borgwardt, 2015), which appeared after the conference publication (Kriege et al., 2014).

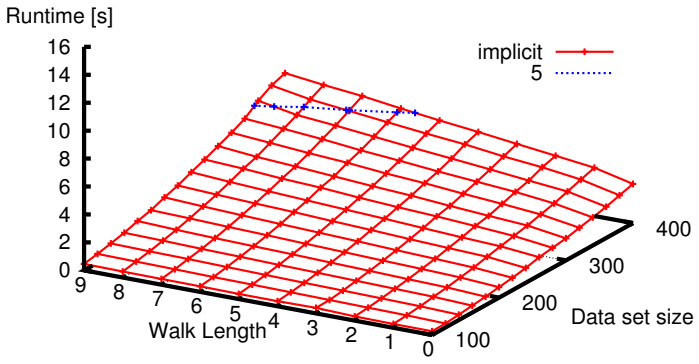


(a) Implicit computation

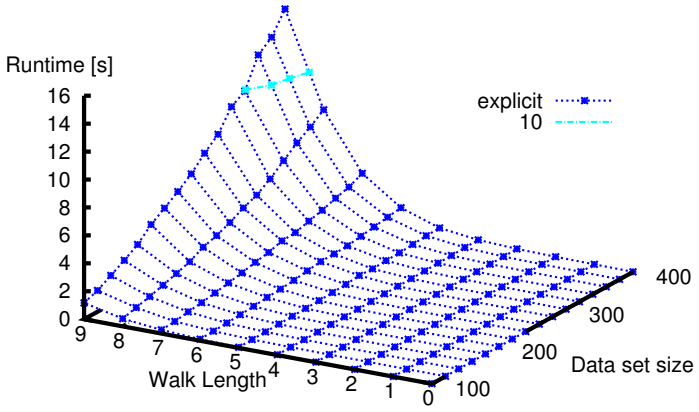


(b) Explicit computation

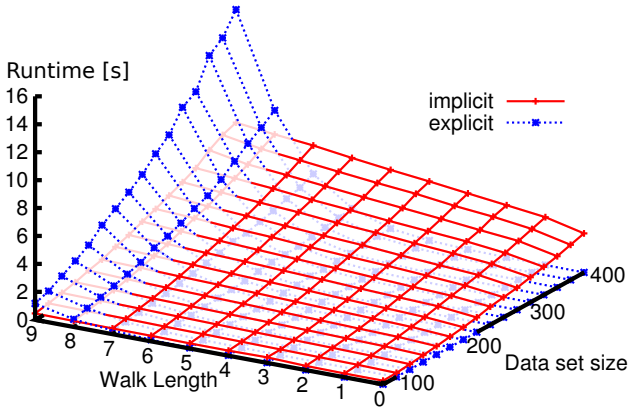


(c) Implicit and explicit computation

Figure 4: Running time to generate the kernel matrix by implicit and explicit computation of walk kernels with varying length for the molecular data set. Figures (a) and (b) show contour lines obtained by linear interpolation.

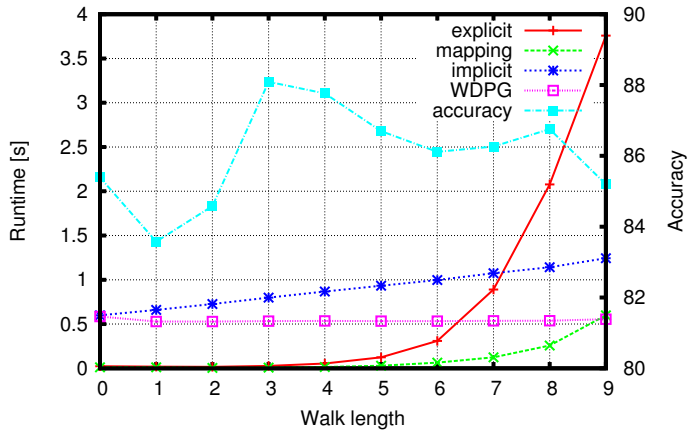


(a) MUTAG

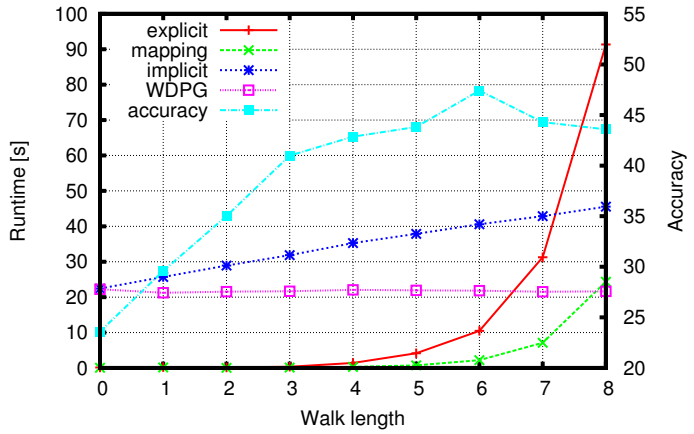


(b) ENZYMES

Figure 5: Running time to generate the kernel matrix and the prediction accuracy on the ENZYMES and MUTAG data sets depending on the walk length.

### 7.3.4 WEISFEILER-LEHMAN LABEL REFINEMENT

Walk kernels have been successfully combined with label refinement techniques (Mahé et al., 2004). We employ the Weisfeiler-Lehman label refinement (WL) as described in Section 6.2.1. To further analyze the sensitivity w.r.t. label diversity, we again use the ENZYMES data set, which consists of graphs with three vertex and two edge labels initially, and apply our algorithms after 0 to 3 iterations of WL, see Figure 6.

If no refinement is applied, the explicit mapping approach beats the product graph based algorithm for the used walk lengths. However, as soon as a single iteration of label refinement is performed, the product graph based algorithm becomes competitive for walk length 0 and 1 and outperforms the explicit mapping approach for higher walk lengths. The running times do not change substantially for more iterations of refinement. This indicates that a single iteration of Weisfeiler-Lehman refinement results in a high label diversity that does not increase considerably for more iterations on the ENZYMES data set. When using our walk-based kernel as base kernel of a Weisfeiler-Lehman graph

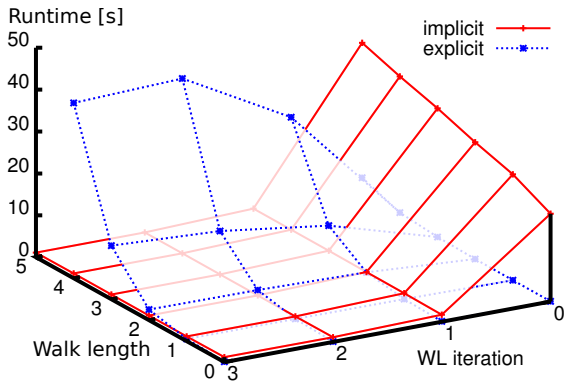


Figure 6: Running time to generate the kernel matrix by implicit and explicit computation of walk kernels with varying walk length and iterations of Weisfeiler-Lehman refinement on the ENZYMES data set.

kernel (Shervashidze et al., 2011), our observation suggests to start with explicit computation and switch to the implicit computation scheme after few iterations of refinement.

#### 7.3.5 SHORTEST-PATH KERNEL

For the shortest-path kernel we found that explicit mapping clearly outperforms implicit computation by several orders of magnitude with respect to running time. This is in accordance with our theoretical analysis and our results suggest to always use explicit computation schemes for this kernel whenever a Dirac kernel is adequate for label and path length comparison. In this case memory consumption is unproblematic, in contrast to the setting discussed in Section 7.2.

### 7.4 Graphlet and Subgraph Matching Kernels for Graphs with Discrete Labels

In this section we experimentally compare the running time of the subgraph matching and the subgraph (or graphlet) kernel as discussed in Section 6.1.2. The explicit computation scheme, which is possible for graphs with discrete labels compared by the Dirac kernel, is expected to be favorable.

The experiments were conducted using Sun Java JDK v1.6.0 on an Intel Xeon E5430 machine at 2.66GHz with 8GB of RAM using a single processor only. The reported running times are average values over 5 runs. We have reimplemented a variation of the graphlet kernel taking connected induced subgraphs with three vertices and discrete vertex and edge labels into account. The only possible features are triangles and paths of length two. Graph canonization is realized by selecting the lexicographically smallest string obtained by traversing the graph and concatenating the observed labels. Our implementation is similar to the approach used by Shervashidze et al. (2011) as extension of the original graphlet kernel (Shervashidze et al., 2009) to the domain of labeled graphs. We refer to this method as graphlet kernel in the following. We compared the graphlet kernel to the connected subgraph matching kernel taking only connected subgraphs on three vertices into account. In order not to penalize the running time of the connected subgraph matching kernel by additional automorphism computations, the weight function does not consider the number of automorphisms (Kriege and Mutzel, 2012, Theorem 2) and, consequently, not the same kernel values are computed.

For real-world instances we observed that explicit computation outperforms implicit computation by several orders of magnitude. This in accordance with our theoretical analysis. However, the practical considerations suggest that explicit and implicit computation behave complementary and subgraph matching kernels become competitive if a sufficient small and sparse weighted product graph is generated, which occurs for graphs with increasing label diversity as for the walk-based kernels. Hence, we randomly generated graphs with the following procedure: The number of vertices was determined by a Poisson distribution with mean $60$. Edges were inserted between a pair of vertices with probability $0.5$. Labels for vertices and edges were assigned with equal probability, whereas the size of the label alphabet $\mathcal{L} = \mathcal{L}_V = \mathcal{L}_E$ is varied from $1$, i.e., uniform labels, to $65$. Note that the graphs obtained by this procedure have different characteristics than those used to show the computational phase transition for walk-based kernels. We vary the data set size $d$ between $100$ and $300$ adding $50$ randomly generated graphs in each step and analyze the running time to compute the $d \times d$ kernel matrix. For the subgraph matching kernel we used the Dirac kernel as vertex and edge kernel.

Figure 7 shows a computational phase transition: For this synthetic data set the subgraph matching kernel is more efficient than the graphlet kernel for instances with 20-30 different labels and its running time increases exponentially when the number of labels decreases. The graphlet kernel in contrast is more efficient for graphs with uniform or few labels. For more than 10 different labels, there is only a moderate increase in running time. This can be explained by the fact that the number of features contained in the graphs does not increase considerably as soon as a certain number of different labels is reached. The enumeration of triangles dominates the running time for this relatively dense synthetic data set. The running time behavior of the subgraph matching kernel is as expected and is directly related to the size and number of edges in the weighted association graph.

Our synthetic data set differs from typical real-world instances, since we generated dense graphs with many different labels, which are assigned uniformly at random. For real-world data sets the graphlet kernel consistently outperforms the subgraph matching kernel by orders of magnitude. It would be interesting to further investigate where this computational phase transition occurs for larger subgraphs and to analyze if the implicit computation scheme then becomes competitive for instances of practical relevance. This requires the implementation of non-trivial graph canonization algorithms and remains future work. The results we obtained clearly suggest to prefer the explicit computation schemes when no flexible scoring by vertex and edge kernels is required.

## 8. Conclusion

The breadth of problems requiring to deal with graph data is growing rapidly and graph kernels have become an efficient and widely used method for measuring similarity between graphs. Highly scalable graph kernels have recently been proposed for graphs with thousands and millions of vertices based on explicit graph feature maps. Implicit computation schemes are used for kernels with a large number of possible features like walks and when graphs are annotated by continuous attributes.

To set the stage for the experimental comparison, we actually made several contributions to the theory and algorithmics of graph kernels. We presented a unified view on implicit and explicit graph features. More precisely, we derived explicit feature maps from the implicit feature space of convolution kernels and analyzed the circumstances rendering this approach feasible in practice. Using these results, we developed explicit computation schemes for random walk kernels (Gärtner et al., 2003; Vishwanathan et al., 2010), subgraph matching kernels (Kriege and Mutzel, 2012),

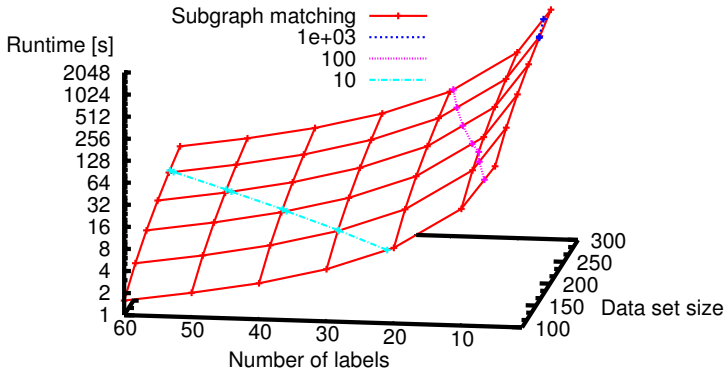


(a) Subgraph matching kernel (implicit)

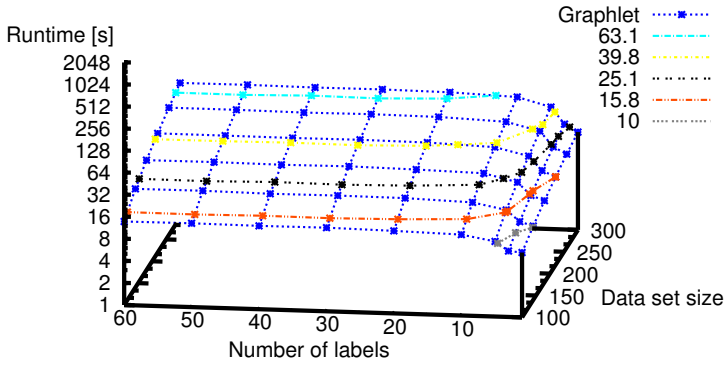


(b) Graphlets with three vertices (explicit)

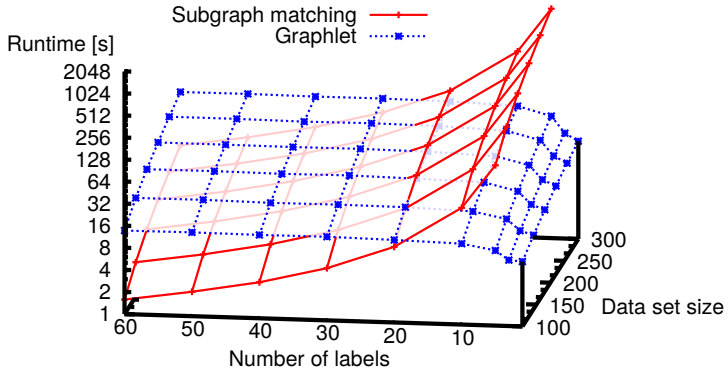


(c) Implicit and explicit computation

Figure 7: Running time to generate the kernel matrix by implicit and explicit computation for synthetic data sets with varying size of the label alphabet. Figures (a) and (b) show contour lines obtained by linear interpolation.

and shortest-path kernels (Borgwardt and Kriegel, 2005). Moreover, we introduced the weighted vertex kernels and derived explicit feature maps. As a result of this we obtained approximate feature maps for state-of-the-art kernels for graphs with continuous attributes like the GraphHopper kernel (Feragen et al., 2013). For fixed length walk kernels we have developed implicit and explicit computation schemes and analyzed their running time. Our theoretical results have been confirmed experimentally by observing a computational phase transition with respect to label diversity and walk lengths.

We have shown that kernels composed by multiplication of non-trivial base kernels may lead to a rapid growth of the number of non-zero components in the feature vectors, which renders explicit computation infeasible. One approach to alleviate this is to introduce hashing of feature dimensions in such cases following the work by Shi et al. (2009).

## Acknowledgments

This work has been supported by the German Science Foundation (DFG) within the Collaborative Research Center SFB 876 "Providing Information by Resource-Constrained Data Analysis", project A6 "Resource-efficient Graph Mining".

## References

A. Andoni. *Nearest Neighbor Search: the Old, the New, and the Impossible*. Phd thesis, MIT, 2009.

L. Bai, L. Rossi, Z. Zhang, and E. R. Hancock. An aligned subtree kernel for weighted graphs. In *Proceedings of the Thirty-second International Conference on Machine Learning*, pages 30–39, 2015.

K. M. Borgwardt and H.-P. Kriegel. Shortest-path kernels on graphs. In *Proceedings of the Fifth IEEE International Conference on Data Mining*, pages 74–81, 2005.

K. M. Borgwardt, C. S. Ong, S. Schönauer, S. V. N. Vishwanathan, A. J. Smola, and H.-P. Kriegel. Protein function prediction via graph kernels. *Bioinformatics*, 21 Suppl 1:i47–i56, 2005.

C.-C. Chang and C.-J. Lin. LIBSVM: A library for support vector machines. *ACM Transactions on Intelligent Systems and Technology*, 2:27:1–27:27, 2011. Software available at `http://www.csie.ntu.edu.tw/~cjlin/libsvm`.

A. Feragen, N. Kasenburg, J. Petersen, M. D. Bruijne, and K. Borgwardt. Scalable kernels for graphs with continuous attributes. In C. Burges, L. Bottou, M. Welling, Z. Ghahramani, and K. Weinberger, editors, *Advances in Neural Information Processing Systems 26*, pages 216–224, 2013. Erratum available at `http://image.diku.dk/aasa/papers/graphkernels_nips_erratum.pdf`.

T. Gärtner, P. Flach, and S. Wrobel. On graph kernels: Hardness results and efficient alternatives. In *Learning Theory and Kernel Machines*, volume 2777 of *Lecture Notes in Computer Science*, pages 129–143. Springer, 2003.

Z. Harchaoui and F. Bach. Image classification with segmentation graph kernels. In *IEEE Conference on Computer Vision and Pattern Recognition*, 2007.

D. Haussler. Convolution kernels on discrete structures. Technical Report UCSC-CRL-99-10, University of California, Santa Cruz, CA, USA, 1999.

S. Hido and H. Kashima. A linear-time graph kernel. In *The Ninth IEEE International Conference on Data Mining*, pages 179–188, 2009.

T. Horváth, T. Gärtner, and S. Wrobel. Cyclic pattern kernels for predictive graph mining. In *Proceedings of the Twelfth ACM SIGKDD International Conference on Knowledge Discovery and Data Mining*, pages 158–167, 2004.

T. Joachims. Training linear SVMs in linear time. In *Proceedings of the Twelfth ACM SIGKDD International Conference on Knowledge Discovery and Data Mining*, pages 217–226, 2006.

U. Kang, H. Tong, and J. Sun. Fast random walk graph kernel. In *Proceedings of the 2012 SIAM International Conference on Data Mining*, pages 828–838, 2012.

P. Kar and H. Karnick. Random feature maps for dot product kernels. In *Proceedings of the Fifteenth International Conference on Artificial Intelligence and Statistics, AISTATS 2012, La Palma, Canary Islands, April 21-23, 2012*, pages 583–591, 2012.

H. Kashima, K. Tsuda, and A. Inokuchi. Marginalized kernels between labeled graphs. In *Proceedings of the Twentieth International Conference on Machine Learning*, pages 321–328, 2003.

K. Kersting, N. M. Kriege, C. Morris, P. Mutzel, and M. Neumann. Benchmark data sets for graph kernels, 2016. URL `http://graphkernels.cs.tu-dortmund.de`.

N. Kriege and P. Mutzel. Subgraph matching kernels for attributed graphs. In *Proceedings of the 29th International Conference on Machine Learning*. 2012.

N. Kriege, M. Neumann, K. Kersting, and M. Mutzel. Explicit versus implicit graph feature maps: A computational phase transition for walk kernels. In *2014 IEEE International Conference on Data Mining*, pages 881–886, 2014.

P. Mahé, N. Ueda, T. Akutsu, J.-L. Perret, and J.-P. Vert. Extensions of marginalized graph kernels. In *Proceedings of the twenty-first international conference on Machine learning*, pages 70–, 2004.

C. Morris, N. M. Kriege, K. Kersting, and P. Mutzel. Faster kernels for graphs with continuous attributes via hashing. In F. Bonchi and J. Domingo-Ferrer, editors, *IEEE International Conference on Data Mining (ICDM)*, 2016. `arXiv:1610.00064`.

M. Neumann, R. Garnett, C. Bauckhage, and K. Kersting. Propagation kernels: Efficient graph kernels from propagated information. *Machine Learning*, 102(2):209–245, 2016.

F. Orsini, P. Frasconi, and L. De Raedt. Graph invariant kernels. In *Proceedings of the Twenty-fourth International Joint Conference on Artificial Intelligence*, pages 3756–3762, 2015.

N. Pham and R. Pagh. Fast and scalable polynomial kernels via explicit feature maps. In *Proceedings of the 19th ACM SIGKDD International Conference on Knowledge Discovery and Data Mining*, KDD '13, pages 239–247, New York, NY, USA, 2013. ACM. ISBN 978-1-4503-2174-7. doi: 10.1145/2487575.2487591.

A. Rahimi and B. Recht. Random features for large-scale kernel machines. In *Advances in Neural Information Processing Systems 20*, pages 1177–1184. 2008.

J. Ramon and T. Gärtner. Expressivity versus efficiency of graph kernels. In *First International Workshop on Mining Graphs, Trees and Sequences*, 2003.

J. Shawe-Taylor and N. Cristianini. *Kernel Methods for Pattern Analysis*. Cambridge University Press, New York, 2004.

N. Shervashidze, S. Vishwanathan, T. H. Petri, K. Mehlhorn, and K. M. Borgwardt. Efficient graphlet kernels for large graph comparison. In *12th International Conference on Artificial Intelligence and Statistics*, 2009.

N. Shervashidze, P. Schweitzer, E. J. van Leeuwen, K. Mehlhorn, and K. M. Borgwardt. Weisfeiler-lehman graph kernels. *Journal of Machine Learning Research*, 12:2539–2561, 2011.

Q. Shi, J. Petterson, G. Dror, J. Langford, A. Smola, and S. Vishwanathan. Hash kernels for structured data. *J. Mach. Learn. Res.*, 10:2615–2637, Dec. 2009. ISSN 1532-4435.

K. Shin and T. Kuboyama. A generalization of Haussler's convolution kernel — mapping kernel and its application to tree kernels. *Journal of Computer Science and Technology*, 25:1040–1054, 2010.

Y. Su, F. Han, R. E. Harang, and X. Yan. A fast kernel for attributed graphs. In *Proceedings of the 2016 SIAM International Conference on Data Mining*, 2016.

M. Sugiyama and K. M. Borgwardt. Halting in random walk kernels. In *Advances in Neural Information Processing Systems 28*, pages 1630–1638, 2015.

S. J. Swamidass, J. Chen, J. Bruand, P. Phung, L. Ralaivola, and P. Baldi. Kernels for small molecules and the prediction of mutagenicity, toxicity and anti-cancer activity. *Bioinformatics*, 21 Suppl 1: i359–i368, Jun 2005. doi: 10.1093/bioinformatics/bti1055.

A. Vedaldi and A. Zisserman. Efficient additive kernels via explicit feature maps. *IEEE Transactions on Pattern Analysis and Machine Intelligence*, 34(3):480–492, 2012.

S. V. N. Vishwanathan, N. N. Schraudolph, R. I. Kondor, and K. M. Borgwardt. Graph kernels. *Journal of Machine Learning Research*, 11:1201–1242, 2010.

N. Wale, I. A. Watson, and G. Karypis. Comparison of descriptor spaces for chemical compound retrieval and classification. *Knowledge and Information Systems*, 14(3):347–375, 2008.